Applied Geochemistry 207 (2026) 106955

Contents lists available at ScienceDirect

Applied Geochemistry

journal homepage: www.elsevier.com/locate/apgeochem

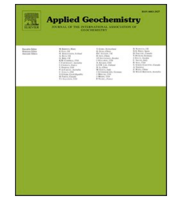

Hydrological convergence and surface–groundwater connectivity are associated with fluorescent groundwater DOM in the Victoria and Kyoga Basins, Uganda

Derick Muloogi [a,b], Daren C. Gooddy [c,1,2], David A. Polya [a], Laura A. Richards [a,*]

[a] Department of Earth and Environmental Sciences and Williamson Research Centre for Molecular Environmental Science, The University of Manchester, Williamson Building, Oxford Road, Manchester, M13 9PL, United Kingdom
[b] Department of Energy, Minerals, and Petroleum Studies, Mbarara University of Science and Technology, P.O Box 1410, Mbarara, Uganda
[c] British Geological Survey, Maclean Building, Wallingford, Oxfordshire, OX10 8BB, United Kingdom

A R T I C L E I N F O

Editorial handling by Elisa Sacchi

Keywords:
Groundwater
Fluorescent dissolved organic matter
Land use/land cover
Topographic wetness index
Surface-groundwater connectivity
East Africa

A B S T R A C T

Dissolved organic matter (DOM) influences subsurface biogeochemistry yet controls on its composition in many tropical sub-Saharan aquifers remain poorly understood. Here, we integrated satellite-derived land-use/land-cover (LULC) data, terrain metrics, and inorganic tracers (NO_3^-/Cl^-, SO_4^{2-}/Cl^-) to evaluate how LULC patterns and terrain-driven hydrological convergence, expressed as topographic wetness index (TWI), influence bulk and fluorescent groundwater DOM (fDOM) across multiple spatial scales in Uganda. Groundwater DOM was dominated by weakly aromatic, highly processed material of mixed terrestrial and microbial origin (specific ultraviolet absorbance (SUVA) < 0.5 L $mg^{-1}.m^{-1}$; median humification index (HIX_{corr}) > 0.5, β:α < 1, and fluorescence index (FI) ~ 1.6). Total fluorescence (0.1 – 12.3 RU; median 0.3 RU) was dominated by fulvic-like (~35 %) and tryptophan-like (~29 %), followed by tyrosine-like (~18 %) and humic-like (~17 %) components. The combined influence of LULC and TWI was scale dependent, although LULC categories showed no significant associations with groundwater DOM, except surface-water cover. TWI was positively associated with dissolved organic carbon (DOC), and fDOM components consistent with potential lateral mobilisation and surface–-groundwater interaction in hydrologically convergent zones. NO_3^-/Cl^- ratios were negatively correlated with DOC (Spearman $\rho \sim -0.56$), and positively with SUVA ($\rho \sim 0.46$), consistent with preferential depletion of relatively bioavailable DOM fractions and relative enrichment of more aromatic residual DOM under nitrate-enriched conditions. These results show that in the Victoria and Kyoga basins, hydrological convergence, rather than land use alone, likely influences groundwater DOM composition, highlighting surface waters and near-surface hyporheic zones as potential sources and transformation environments for organic matter entering aquifers.

1. Introduction

Dissolved organic matter (DOM) is the main mobile reservoir of organic carbon in freshwaters, influencing global carbon cycling, nutrient transport, and contaminant mobility (Aiken et al., 2011; Findlay and Sinsabaugh, 2003). In groundwater, DOM originates from both autochthonous sources, such as microbial exudates, and allochthonous inputs from plant litter and soil- or sediment-derived organic matter (Fellman et al., 2010; Harjung et al., 2023; Shen et al., 2015). DOM composition can reflect land use (Gad et al., 2024; Williams et al., 2010; Wilson and Xenopoulos, 2009), hydrological connectivity, and recharge dynamics (Lapworth et al., 2009; Lynch et al., 2019; Townsend-Small et al., 2011; Wilson et al., 2023). Yet, despite its important role in subsurface biogeochemistry, the sources, composition, and controls of groundwater DOM remain poorly understood (Chen et al., 2010; Saito et al., 2023; Shen et al., 2015), particularly in sub-Saharan tropics, including Uganda, where rapid land conversion and limited data constrain understanding of surface–groundwater

* Corresponding author.
E-mail address: laura.richards@manchester.ac.uk (L.A. Richards).
[1] Current: UKCEH, Maclean Building, Wallingford, Oxfordshire, OX10 8BB, United Kingdom.
[2] Current: Lancaster Environment Centre, Lancaster University, Lancaster, LA1 4YQ, United Kingdom.

https://doi.org/10.1016/j.apgeochem.2026.106955
Received 26 February 2026; Received in revised form 23 June 2026; Accepted 23 June 2026
Available online 24 June 2026
0883-2927/© 2026 The Authors. Published by Elsevier Ltd. This is an open access article under the CC BY license (http://creativecommons.org/licenses/by/4.0/).

carbon dynamics.

Land-use and land-cover (LULC) changes, driven by agricultural expansion and urbanisation, can alter both the DOM quantity and composition in aquatic environments (Catipovic et al., 2026; Williams et al., 2016; Xenopoulos et al., 2021). Agricultural catchments typically export more microbially derived, protein-like DOM (Williams et al., 2010; Wilson and Xenopoulos, 2009), whereas urban catchments contribute higher proportions of anthropogenic fulvic-like and protein-like signatures (Hosen et al., 2014). The extent to which these surface-derived signals propagate into groundwater, however, depends critically on hydrological connectivity and the subsequent biogeochemical transformation within the subsurface (McDonough et al., 2022). In tropical regions characterised by dense drainage networks, open waters, and shallow aquifers, lateral and vertical exchanges can enhance DOM transfer from surface water to groundwater, particularly where abstraction, drainage, or land modification alter recharge pathways (Lawson et al., 2013; Neumann et al., 2010; Wilson et al., 2023).

Surface–subsurface connectivity comprises structural and functional components. Structural connectivity reflects relatively static landscape attributes, such as topography, soil, and vegetation, that define potential flow pathways, whereas functional connectivity describes the transient activation of those pathways during rainfall or recharge events (Bracken et al., 2013; Dwivedi et al., 2025). Among structural controls, terrain-driven flow is especially important in directing runoff and solute transport into low-lying, hydrologically active zones (Burt and Pinay, 2005). The Topographic Wetness Index (TWI) offers a physically-based measure of such convergence, integrating local slope and upslope contributing area to identify sites with higher potential for water accumulation and lateral redistribution (Beven and Kirkby, 1979; Quinn et al., 1991; Sørensen et al., 2006). As a static, topography-based index, TWI reflects structural hydrological connectivity rather than functional or event-driven flow. High TWI values indicate areas prone to sustained wetness and enhanced subsurface exchange, while low values correspond to well-drained sites. These hydrologically convergent, high-TWI settings typically correspond to riparian corridors, wetlands, and shallow subsurface zones, including hyporheic regions adjacent to streams (Lang et al., 2013). In these zones, organic matter and solutes are mobilised, mixed, and partially transformed before entering groundwater (Lapworth et al., 2009; Lynch et al., 2019; Stegen et al., 2016). Because of its sensitivity to terrain-controlled hydrology, TWI has been applied to predict groundwater levels (Rinderer et al., 2014; Sørensen et al., 2006), groundwater recharge potential (Balasubramaniyan et al., 2025), hydrological connectivity (Epting et al., 2018; Jancewicz et al., 2019; Pavlin et al., 2021), soil moisture, and soil organic carbon distribution (Kopecký et al., 2021; Obu et al., 2017; Pei et al., 2010; Riihimäki et al., 2021). However, the relationships between terrain-mediated connectivity and groundwater DOM composition remain poorly characterised.

In Uganda, shallow aquifers predominantly underpin both rural and peri-urban water supplies but are increasingly stressed by dense settlements, agricultural expansion, and extensive surface waters (Muloogi et al., 2026, 2025; MWE, 2025; UBOS, 2024). These pressures are reflected in elevated nutrient loads, particularly NO_3^- and SO_4^{2-} (Nyenje et al., 2013, 2014; Wilson et al., 2024b), which typically co-occur with DOM. DOM in these nutrient-rich aquifers may originate from surface-derived inputs transported alongside nutrients or may be produced *in-situ* and modified through microbial processing within the subsurface (Wilson et al., 2024a, 2024b). Such pathways and interactions may occur across Uganda's diverse hydrological basins, especially in the Victoria and Kyoga basins, where dynamic surface water–groundwater exchange occurs (Kayendeke and French, 2019; Owor et al., 2011), providing a conduit for ingress of surface-origin solutes and DOM into the aquifers. In these hydrologically-connected landscapes, terrain-driven flow convergence can amplify the effects of surface activities on groundwater quality by funnelling surface-derived contaminants and organic matter into recharge zones. Understanding how these hydrological conditions and anthropogenic activities jointly influence groundwater DOM is therefore essential for delineating the source, transformations, and fate of organic carbon in Uganda's aquifers amidst the intensifying human pressures.

Fluorescence spectroscopy provides a powerful means of understanding these processes through rapid, cost-effective, non-destructive, and sensitive characterisation of groundwater DOM (Moore et al., 2024; Richards et al., 2019; Wilson et al., 2023, 2025). Excitation-emission matrices (EEMs) allow differentiation of humic- and protein-like fractions, typically associated with terrestrial and microbial origins, respectively (Coble, 1996; Yamashita et al., 2008), while fluorescence-derived indices, including the humification (HIX; Ohno, 2002), biological (BIX; Huguet et al., 2009), and fluorescence (FI; Cory and McKnight, 2005; McKnight et al., 2001) indices, provide complementary insights into DOM age, processing, and origin. This approach has proven effective in tracing groundwater flow paths (Baker and Lamont-BIack, 2001; Lapworth et al., 2008), assessing groundwater–surface water interactions (Lapworth et al., 2009), and identifying contamination from agricultural waste, sewage, and landfill leachates (Baker, 2001, 2002; Baker and Curry, 2004). However, despite this potential, its application to understanding land–hydrology–DOM interactions, particularly in relation to surface–groundwater connectivity in sub-Saharan aquifers, remains limited, leaving the biogeochemical imprints of surface influence on tropical groundwater DOM in regions such as Uganda largely unresolved.

Here, we hypothesised that: (1) groundwater DOM composition in Uganda reflects combined influence of LULC and terrain-driven surface–groundwater connectivity across multiple spatial scales; (2) protein-like, anthropogenic DOM fractions are higher in cropland and urban environments than in less disturbed environments; and (3) NO_3^-/Cl^- and SO_4^{2-}/Cl^- ratios serve as indicators of localised surface-derived contamination and are associated with shifts in groundwater DOM composition, possibly linked to microbial processing under nutrient-enriched conditions. By integrating LULC data, topographic wetness indices, fluorescent DOM (fDOM), bulk DOC, and inorganic tracers from groundwater and surface water across the Victoria and Kyoga basins in eastern and central Uganda, this study provides the first regional characterisation of groundwater DOM in Uganda and demonstrate a transferable methodology for linking land use–hydrology–DOM interactions across aquifers with comparable hydroclimatic regimes.

2. Methodology

2.1. Study area

2.1.1. Regional setting

Uganda covers ~241,000 km^2, of which 15 – 16 % is surface water (NEMA, 2016; UN-WWAP, 2006). Nearly 98 % of the country's territory drains into the Nile Basin, which is administered nationally through eight hydrological basins: Lake Victoria, Lake Kyoga, Victoria Nile, Lake Albert, Lake Edward, Albert Nile, Achwa, and Kidepo (DWRM, 2014; USAID-SWP, 2021).

This study focused on central and eastern Uganda, primarily within the Lake Victoria and Lake Kyoga basins (Fig. 1). Lake Victoria connects to Lake Kyoga through the White Nile and associated tributaries, forming an extensive river–lake network that underpins much of Uganda's hydrology (Nsubuga et al., 2014). The study area further extends north-eastward from Mt. Elgon, encompassing varied landscapes and land-use patterns that could potentially influence DOM dynamics in surface and groundwaters.

2.1.2. Land-use and land-cover context

Agriculture dominates the land-use categories across Uganda. Smallholder systems produce maize, bananas, cassava, and beans, while sugarcane, coffee, and tea are cultivated commercially within the Lake Victoria and Lake Kyoga basins (Forest Trends, 2024). Fertiliser

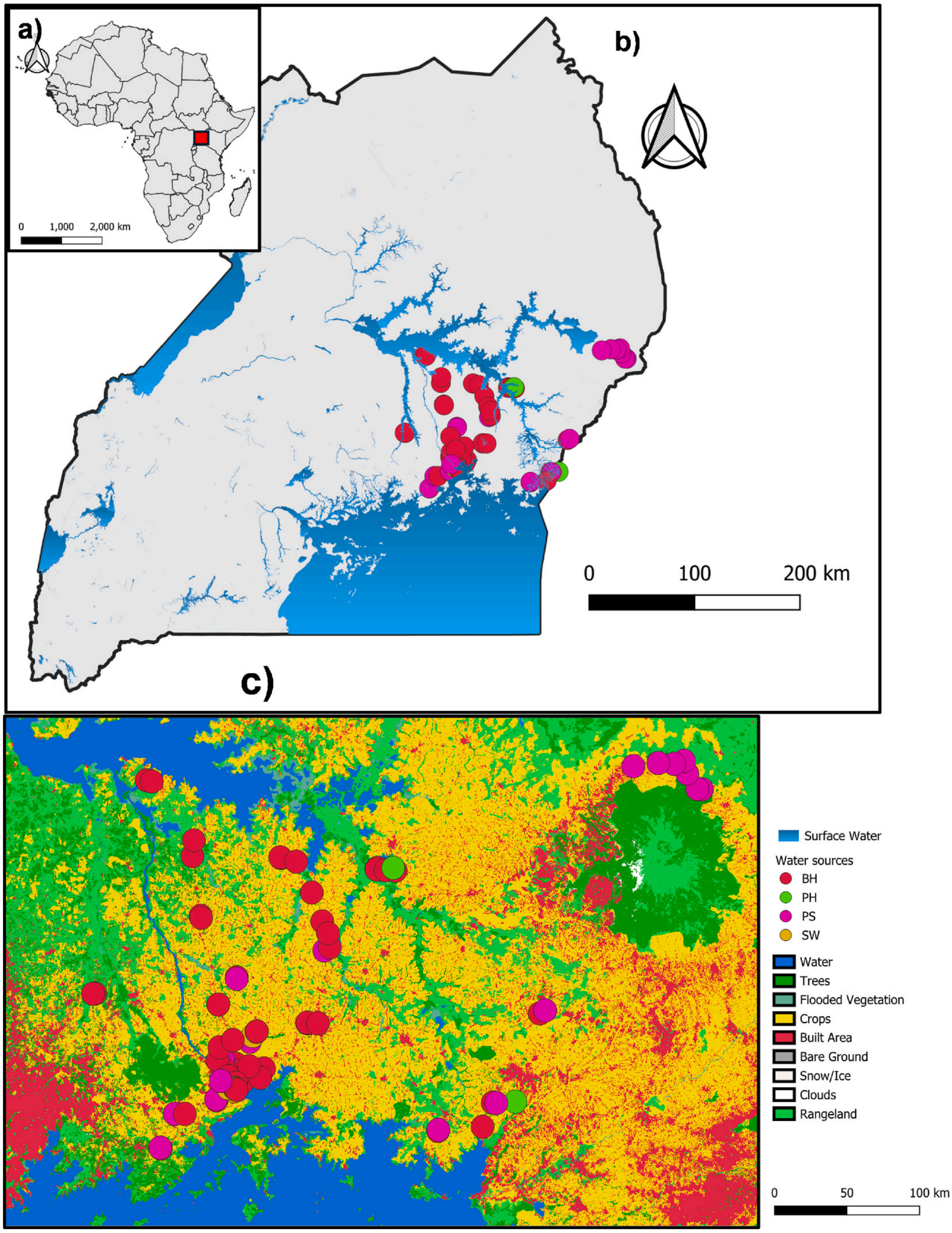

Fig. 1. Maps showing (**a**) Uganda's location in Africa, (**b**) the sampling sites (Groundwater (n = 72); Surface water (n = 8)), and (**c**) the distribution of sites across the different Land-use Land-cover classes represented by the different colour bands. The corresponding maps were created based on the following shape files: A (ICPAC, 2017); B (OCHA, 2020); and C (Esri, 2023). The colour codes represent the different water sources sampled: BH – Borehole, PH – Piped groundwater supply system, SW – Surface water, PS – Protected Spring). (For interpretation of the references to colour in this figure legend, the reader is referred to the Web version of this article.)

application remains modest (1 – 2.5 kg $ha^{-1}.yr^{-1}$, mainly NPK 17:17:17), though drastically increasing over time (IFDC, 2018; MAAIF, 2016).

Agricultural expansion, deforestation, and wetland encroachment are reshaping the landscape and could potentially alter organic and nutrient fluxes to aquatic environments (Xenopoulos et al., 2021). Between 2002 and 2024, Uganda's primary forest cover declined by ~16 %, largely due to agricultural conversion, logging, and urbanisation (GFW, 2024). Wetlands, comprising swamps, floodplains, and riparian zones, have decreased by ~30 % since the 1990s (UNEP, 2009). Recent Sentinel-2 (10 m) LULC data (Esri, 2023) indicate dominant coverage by crops (45 – 50 %), followed by grasslands (15 – 20 %), water (15 – 18 %), trees (12 – 15 %), shrubs (5 – 8 %), flooded vegetation (3 – 5 %), built-up areas (2 – 4 %), and bare ground (1 – 2 %).

2.1.3. *Topography and hydrological context*

Uganda's elevation ranges from roughly 900 – 1500 m a.s.l. across the central plateau to over 3000 m in isolated highlands (Lyons et al., 2025). In eastern Uganda, the terrain grades from gently rolling plateaus to the volcanic uplands surrounding Mt. Elgon, whose radial drainage sends flow in multiple directions. North-ward flowing rivers such as the Suam drain across the international border into Kenya and the Turkana basin, while the western and northwestern slopes generate the Sipi, Sironko, and Simu rivers that flow into tributaries of the Lake Kyoga (Nsubuga et al., 2014). To the south and southwest, catchments including the Manafwa, Lwakhakha, and Malaba rivers drain towards Lake Victoria basin. These uplands merge downslope into extensive low-gradient plains and wetland complexes that redistribute flow locally within the Kyoga basin, producing internally drained and diffuse patterns. South of this zone, the landscape gently inclines towards the Lake Victoria basin, characterised by subdued topography and thick weathering profiles (Owor et al., 2011). Flow orientations here are locally variable but generally converge southward into Lake Victoria, which discharges northward to Lake Kyoga via the Victoria Nile.

In the absence of extensive hydraulic head data, large-scale groundwater flow directions were inferred from topographic gradients and regional slope analyses. Across the entire study area, flow-direction analysis shows a broadly bimodal orientation: northeast and southwest (Fig. 2). The northeast dominance reflects the broad regional slope of the central plateau towards the Lake Kyoga depression, while the southwest component follows gradients draining towards the Lake Victoria catchment. The intervening plains and wetland corridors create locally variable flow directions consistent with low relief. These dense drainage networks, especially within the Kyoga basin, promote localised infiltration, influenced by locally variable slopes, soil depth and land use (Kayendeke and French, 2019; Namaalwa et al., 2020; Obubu et al., 2022).

2.1.4. *Climate*

Uganda experiences a tropical bimodal rainfall regime, with major wet seasons from March–May and September–November, separated by drier periods. Mean annual rainfall exceeds 2000 mm near Lake Victoria, western highlands, and Mount Elgon, declining to <700 mm in the semi-arid north. Temperatures are relatively stable year-round, averaging 22 – 24 °C. Daytime maxima typically reach 26 – 27 °C in the central plateau and lowlands, while highland areas, including regions around Mt. Elgon, are slightly cooler, with maxima around 22 – 25 °C (UNMA, 2024).

2.1.5. *Hydrogeology and recharge*

The study region is hydrogeologically diverse but is predominantly underlain primarily by Precambrian crystalline basement rocks (BGS, 2019). Productive aquifers occur within secondary structures, including weathered regolith, fractures, and the saprolite–bedrock interface (Owor et al., 2018), and typically yield modest groundwater due to limited transmissivity (Owor et al., 2018). Groundwater recharge is largely meteorologically driven, occurring via direct infiltration through deeply weathered zones and through focused flow along rivers and stream channels, particularly where overland flow is substantial (Howard and Karundu, 1992; Taylor and Howard, 1996).

2.2. *Sample collection*

Water was sampled in February/March 2024 from boreholes ($n = 49$), protected springs ($n = 20$), piped groundwater supply system ($n = 3$) and surface water ($n = 8$). All boreholes and piped groundwater supplies were in frequent and regular use and were purged for ~2 min to obtain representative aquifer samples. Groundwater samples were collected from communities' domestic water points across various districts in eastern and central Uganda, including Iganga, Kaliro, Tororo, Jinja, Buikwe, Kibuku, Kamuli, Buyende, Kayunga, Kween, Bukwo, Kapchorwa, and Busia, covering parts of both the Victoria and Kyoga basins. Surface waters were collected from Lake Victoria ($n = 4$), Nile River ($n = 2$) and ponds ($n = 2$) within and around Jinja city to represent the regional surface-water end-members.

Samples for fDOM, DOC, and anion (Cl^-, NO_3^-, and SO_4^{2-}) analyses were filtered *in-situ* through 0.45 μm cellulose syringe filters (Minisart®) and were unacidified. The fDOM samples were stored in 20 mL amber glass bottles filled to the top, while DOC and anion samples were stored in 60 mL glass bottles; all bottles were sealed with Parafilm. All bottles were pre-cleaned prior to sampling by acid-washing in 10 % nitric acid for ~24 h, rinsed thoroughly with MilliQ®-grade deionised water and furnaced at 450 °C.

Sampling replicates (~6 % of total samples) were included to assess sampling consistency. All samples were stored at ~4 °C until analysis, except when this was not possible (*e.g.,* during transit and power outages), to minimise potential changes in organic matter composition (Richards et al., 2019).

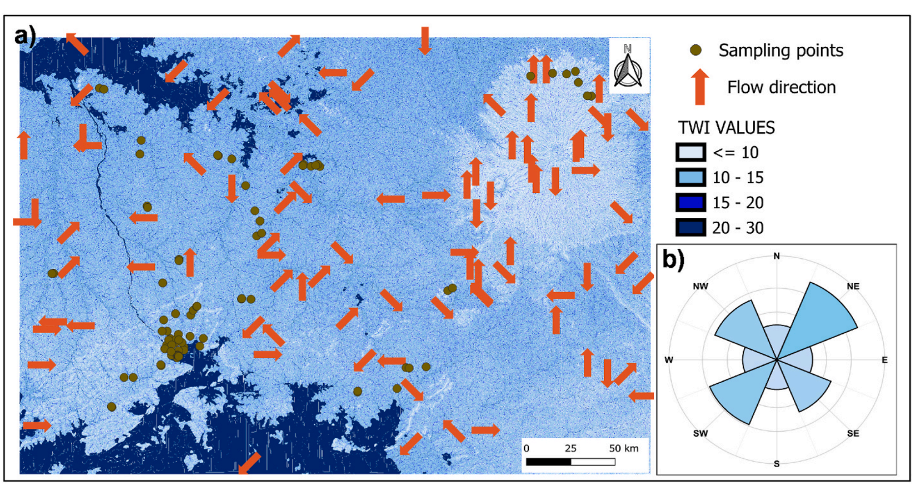

Fig. 2. (a) Topographic Wetness Index (TWI) and sampled sites across eastern and central Uganda, within the Lake Kyoga and Victoria basins, overlaid with local flow orientations derived from a hydrologically corrected Shuttle Radar Topographic Mission (SRTM) digital elevation model (1-arc-second, 30 m; resampled to ~ 90 m) using the D_8 single-flow routing algorithm in WhiteboxTools (Lindsay, 2016). Arrows indicate inferred dominant local flow directions. **(b)** Rose diagram summarising flow-direction frequency across the region, indicating a relatively diffuse pattern with a weakly bimodal orientation towards the northeast and southwest. The northeast component reflects the regional slope from the central plateau into the Lake Kyoga depression, while the southwest component corresponds to gentle gradients draining towards the Lake Victoria catchment. Flow directions in intervening plains and wetlands are highly variable, consistent with the undulating nature of the terrain.

2.3. Sample analysis and quantification

2.3.1. DOC quantification

DOC, measured as non-purgeable organic carbon (NPOC), was analysed at the Manchester Analytical Geochemical Unit (MAGU) using a Shimadzu® TOC-VCPN Total Organic Carbon Analyzer with an ASI-V autosampler and 24 mL glass vials. Detection was based on combustion catalytic oxidation method at 680 °C (Sugimura and Suzuki, 1988). Several samples ($n = 9$) were analysed in replicate to assess analytical precision.

2.3.2. Quantification of anions

Anions (Cl^-, NO_3^-, and SO_4^{2-}) were analysed via ion chromatography (IC; Dionex ICS5000 Ion Chromatograph with Dionex IonPac AS18 columns) at MAGU. Data quality assurance and quality control was previously detailed (Muloogi et al., 2026).

2.3.3. Fluorescence measurements

Optical analyses were conducted at the British Geological Survey laboratory (Wallingford, UK) in March 2024 following methodology previously described (Lapworth and Kinniburgh, 2009; Richards et al., 2019). Fluorescence analysis, conducted with a Varian Cary Eclipse spectrometer, used Excitation (Ex) scanning range of 200 – 400 nm (5 nm bandwidth) and Emission (Em) wavelengths of 250 – 500 nm (2 nm bandwidth) at a photomultiplier tube (PMT) voltage of 725 V. Results, averaged over three repeats, were blank-corrected, normalised to Raman Units, and reported relative to the ultrapure water Raman peak (Ex 350 nm, Em 397 nm). The UV absorbance at 254 nm ($Abs_{254;}$ m^{-1}) was measured using a Varian UV/visible spectrophotometer, and SUVA ($L.mg^{-1}.m^{-1}$) was calculated as Abs_{254}/DOC in $mg.L^{-1}$ (Weishaar et al., 2003), as a proxy for DOM aromaticity, with lower values generally indicating lower aromatic carbon content.

Following data processing, reference peaks of the EEM were quantified, and fluorescence indices calculated using standard peak-picking techniques to infer DOM structure, source and processing. Peak-picking was chosen over parallel factor analysis (PARAFAC) because many groundwater samples had low DOC and weak fluorescence, conditions under which PARAFAC models can be unstable or sensitive to noise (Murphy et al., 2013). Moreover, previous groundwater studies have reported strong correlations between PARAFAC and peak-picked components (Richards et al., 2019; Wilson et al., 2023). Peak-picking was performed for the predefined EEM values corresponding to tryptophan-like (TPH-like), tyrosine-like (TYR-like), fulvic-like, and humic-like fluorescence (Coble, 1996). The fluorescence indices were calculated based on the peak-picked fluorescence intensities: (i) Fluorescence index (FI; for terrestrial vs. microbial DOM, with higher values indicating greater microbial contribution; Cory and McKnight, 2005; McKnight et al., 2001), (ii) HIX corrected for inner filtering (HIX_{corr}), as an indicator of DOM humification and molecular complexity, with higher values reflecting more humified and processed organic matter (Ohno, 2002), (iii) the freshness index (β:α; for labile vs. recalcitrant DOM, where higher values indicate greater DOM freshness and lability; Huguet et al., 2009; Parlanti et al., 2000), and iv) and Tryptophan: Fulvic acid ratio (TPH:FA; as an indicator of proteinaceous relative to fulvic-like DOM contributions, often associated with anthropogenic (sewage) contributions; Baker, 2002, 2001).

2.4. Land-use/land-cover (LULC) data acquisition

Land-use and land-cover data for Uganda were obtained from the Esri Sentinel-2 10 m LULC Time Series, available via the ArcGIS Living Atlas of the World (https://livingatlas.arcgis.com/landcover/). This dataset provides annual 10 m resolution rasters, with each pixel classified into one of nine categories: Built, Crops, Trees, Water, Rangeland, Flooded Vegetation, Snow/Ice, Bare Ground, and Clouds. The 2023 annual composite was used, representing conditions across January to December 2023, immediately preceding sampling.

2.5. Buffer design and LULC quantification

To evaluate the spatial influences of surrounding LULC on groundwater DOM, circular buffers with radii of 50, 100, 200, 250, 500, 700, and 1000 m were created around each groundwater sampling location ($n = 72$). These buffer sizes capture both local (50–250 m) and broader (500–1000 m) spatial scales, consistent with those applied in previous hydrological and land use–water quality studies (Sadeghi Goarbandi et al., 2024; Shi et al., 2017; Song et al., 2020). Surface water sites were excluded from this analysis and retained only for separate comparisons, as their near-complete pixel coverage by water would mask land-cover signals relevant to groundwater DOM. Within each buffer, the proportion of each land-cover class was computed and expressed as its percentage of the total land area. Corrected buffer proportions accounting for focal area bias (Huck et al., 2025) were compared with uncorrected values; as model outcomes were unaffected, uncorrected values were used in all subsequent analyses.

To identify the radius of maximum explanatory power, adjusted R^2 and permutation p-values were compared across the spatial buffer scales (Fig. S1). At the optimal scale, variance partitioning was used to quantify the unique and shared contributions of LULC composition and topographic wetness to DOM variability (Fig. S2).

2.6. Topographic wetness and flow metrics

The topographic wetness index (TWI) was derived from the 30 m Shuttle Radar Topography Mission (SRTM 1 Arc-Second) digital elevation model. The DEM was hydrologically corrected to remove spurious depressions (*WhiteboxTools* v2.4.0; Lindsay, 2016), after which, the slope and D_8 flow accumulation were used to calculate:

$$TWI = \ln\left(\frac{\alpha}{\tan\beta}\right) \quad [1]$$

where α is the upslope contributing area (m^2; proportional to the specific catchment area when normalised by grid-cell width) and β is the local slope (radians) (Beven and Kirkby, 1979). Mean TWI values within each spatial buffer scale were extracted as structural proxies representing the relative potential for surface and subsurface convergence. Flow-directions were also generated from the corrected DEM to visualise inferred dominant local flow pathways across the study region (Fig. 2).

2.7. Relating LULC and topographic wetness to groundwater DOM

Redundancy analysis (RDA) in R v4.3.2 (*vegan* package; Oksanen et al., 2025) was used to assess if/how LULC composition and topographic wetness jointly explain variation in groundwater DOM. Because the LULC data are compositional, proportional values were Hellinger-transformed to stabilise variance, down-weight rare categories, and make them suitable for linear ordination (Legendre and Gallagher, 2001). Low-prevalence LULC classes (<5 % of sites; bare ground, rangeland and flooded vegetation) were excluded to reduce collinearity and improve model stability. Mean TWI values were standardised (mean = 0, variance = 1) and combined with transformed land-cover data to form the predictor matrix for each buffer radius.

The response matrix comprised z-standardised DOM metrics: dissolved organic carbon (DOC), and three fluorescence-derived components (TPH-like, humic-like, and fulvic-like fluorescence). For each buffer radius, models of the form: *DOM metrics ∼ LULC composition + TWI* were fitted. Significance was assessed with 999 Monte Carlo permutations, and model fit evaluated using adjusted R^2 and variance-inflation factors (VIF) (Manly, 2018). Relationships between TWI and bulk and fluorescent DOM components were further explored using Spearman rank correlations and generalised linear models (GLMs).

Confidence intervals (95 % CI) for GLM regression coefficients were estimated using profile likelihood.

Group differences (LULC classes and water-source types) were assessed using Kruskal–Wallis tests or Wilcoxon rank-sum tests, followed by Dunn's post-hoc pairwise comparisons where appropriate. P-values were adjusted using the Benjamini–Hochberg false discovery rate (FDR) correction.

3. Results

3.1. Data quality

Data quality for the anions was previously reported (Muloogi et al., 2026); Cl^-, and NO_3^- were within ±10 % CRM-based analytical bias, while SO_4^{2-} had a bias of −15 %, and was corrected as described therein. Analytical precision for Cl^-, NO_3^-, and SO_4^{2-} was high (coefficients of variation, CV = 1 – 5 %), while sampling repeatability was more variable, ranging from 18 ± 34 % for NO_3^- and to 28 ± 56 % for SO_4^{2-}. Ionic ratio errors reflected comparable trends between analytical and field replicates, with NO_3^-/Cl^- ratios showing analytical and sampling repeatability of 1 ± 1 % and 18 ± 34 %, respectively, and SO_4^{2-}/Cl^- ratios showing 0 % and 28 ± 55 % (Table S1). For DOC, analytical and sampling precision (CV) were 15 % ($n = 9$) and 7 % ($n = 5$), respectively. Optical measurements showed moderate analytical repeatability ($n = 8$), with CVs of 17 % for Abs_{254} and 4 – 20 % across the suite of fDOM components (Table S1). Sampling repeatability for fDOM parameters ranged from 4 to 28 %, with the largest variability observed in TRY-like fluorescence, consistent with expected analytical uncertainties at low DOM levels.

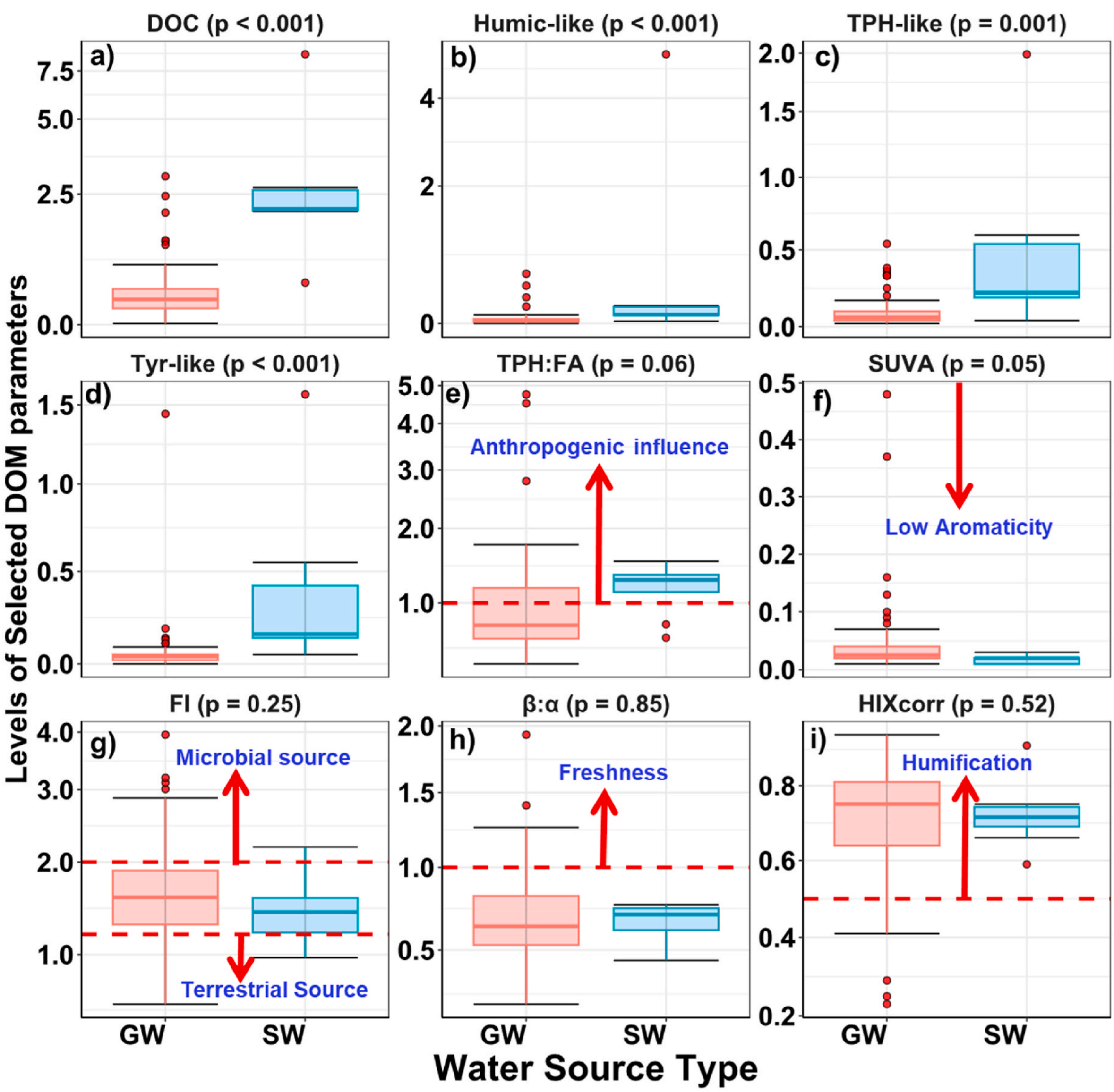

Fig. 3. Boxplots comparing DOM parameters between groundwater (GW; $n = 72$) and surface water (SW; $n = 8$) sources. Parameters include (**a**) dissolved organic carbon (DOC; mg/L), (**b**) humic-like (RU), (**c**) tryptophan-like (TPH-like; RU), (**d**) tyrosine-like (TYR-like; RU) components, (**e**) tryptophan-to-fulvic ratio (TPH: FA), (**f**) SUVA, (**g**) fluorescence index (FI), (**h**) β:α ratio, and (**i**) humification index (HIX_{corr}). Boxplots display medians, interquartile ranges, and outliers (red circles). Dashed red lines indicate reference source thresholds for selected parameters (FI at 1.2 and 2.0 (Cory and McKnight, 2005); β: α at 1.0 (Huguet et al., 2009); HIX_{corr} at 0.5 (Ohno, 2002); and TPH: FA at 1.0 (Baker, 2001, 2002). Red arrows show whether samples lie above or below the reference thresholds. P-values from Wilcoxon rank-sum tests comparing GW and SW are shown above each boxplot to indicate the statistical significance of differences between water sources. (For interpretation of the references to colour in this figure legend, the reader is referred to the Web version of this article.)

3.2. DOM optical and fluorescence properties

3.2.1. DOM characteristics

DOM composition varied across sampled sites in the overall dataset (Tables S1 and S2). DOC spanned over two orders of magnitude (0.02 – 8.6 mg L^{-1}; median = 0.5 mg L^{-1}), paralleled by broad variation in fluorescence components. Total fluorescence ranged from 0.1 to 12.3 RU (median = 0.3 RU), with fluorescence dominated by fulvic-like and protein-like components. Fulvic-like fluorescence accounted for the largest fraction of total fluorescence (11 – 50 %; median = 35 %), followed by TPH-like (13.1 – 73 %; median = 29 %), TYR-like (0 – 47.4 %; median = 18 %), and humic-like components (0 – 44 %; median = 17 %). Low aromaticity indices (SUVA = 0.01– 0.5 L $mg^{-1}.m^{-1}$; median = 0.02 L $mg^{-1}.m^{-1}$) and weak absorbance at 254 nm (0 – 0.5 m^{-1}; median = 0.01 m^{-1}) indicate that much of the DOM was optically dilute and dominated by weakly aromatic material with mixed terrestrial and microbial signatures (Chin et al., 1994; Weishaar et al., 2003).

3.2.2. Fluorescence indices

Fluorescence indices reflect a compositionally mixed DOM pool. The fluorescence index (FI = 0.5 – 4.0; median 1.6) and β:α ratio (0.2 – 1.9; median 0.7) indicated variable contributions of terrestrial and microbial sources, while the TPH:FA ratio (0.3 – 4.7; median 0.8) and corrected humification index (HIX_{corr} = 0.2 – 0.9; median 0.7) point to a predominance of terrestrially derived but processed material (Gabor et al., 2014).

3.3. Comparison between groundwater and surface water fDOM characteristics

Surface waters contained significantly higher DOC, humic-, TPH-, and TYR-like components (all $p \leq 0.001$) than groundwater (Fig. 3; Table S1). The relatively high bulk and fluorescent DOM in surface waters likely reflects the organic loads in major regional surface water bodies, including Nile River and Lake Victoria, all of which were sampled within and around the industrial-dominated Jinja city. Whilst the surface-water sites sampled are not intended to represent the full diversity of surface waters across the basins, they provide plausible regional end-members for major surface-water bodies interacting with groundwater in the study area.

Groundwater showed greater within-source variability in DOM parameters than surface waters (Levene's test: F = 11.8, $p < 0.001$), consistent with spatial heterogeneity in land-use, recharge, and subsurface conditions. When groundwater samples were further stratified by the presence of surface water within a local buffer (cf. Fig. S3), sites with surface water exhibited slightly elevated bulk DOC and fDOM components relative to groundwater without nearby surface water, although values remained lower than in surface waters. TPH:FA ratios were also higher in surface waters, although the difference was not significant (p = 0.06). SUVA was slightly higher in surface waters (p = 0.05) but remained low overall (<0.5 L $mg^{-1}.m^{-1}$) in both sources, reinforcing the weak overall aromaticity across waters. Other optical indices (FI, β:α, HIX_{corr}) showed no significant differences between the groundwater and surface waters (all $p > 0.2$), implying broadly similar sources, microbial and humification characteristics.

Stratification of groundwater by source type revealed significant differences in TPH:FA (p = 0.01), SUVA (p = 0.01), FI (p = 0.007), and β:α (p = 0.003), whereas DOC, humic-like, TPH-like, TYR-like, and HIX_{corr} did not differ significantly among source types (all $p \geq 0.05$; Fig. S4). Pairwise comparisons (Dunn's test, FDR-adjusted) identified protected springs as the main group differing from other groundwater sources. Relative to boreholes, protected springs exhibited higher humic-like signals (p = 0.04) but lower TPH: FA (p = 0.011), FI (p = 0.02), and β:α (p = 0.002). FI was also lower in protected springs than piped groundwater systems (p = 0.02). These patterns suggest broad compositional overlap between surface and groundwater DOM, whilst also highlighting distinct DOM signatures among groundwater source types, likely reflecting differences in flow paths, connectivity and transformation processes during infiltration.

3.4. Influence of LULC on groundwater fDOM patterns

3.4.1. Optimal buffer scale with maximum explanatory power for DOM variability

The 500 m buffer scale showed the highest, though modest, statistically significant explanatory power for groundwater bulk DOC and fDOM variability (p = 0.03; deviance explained = 22 %; adj. R^2 = 0.14; Fig. S1). Smaller buffers (≤250 m) yielded low or negative adjusted R^2 values, which may reflect limited spatial extent captured at these scales, while larger ones (700 m and 1000 m) weakened the explanatory power, potentially due to inclusion of zones beyond the local recharge area, diluting local signals. The highest explanatory power at 500 m radius suggests that this scale integrates the local and upslope landscape influences relevant to groundwater DOM variability. Importantly, the direction of associations and the relative contribution of key predictors to explained variance in the RDA were consistent across multiple buffer sizes, indicating that the observed relationships are not specific to a single radius. Variance Inflation Factor (VIF; 1–6) for the 500 m buffer indicated no significant multicollinearity issues. Within this buffer, dominant LULC types were cropland (CL, n = 36; 50 %), followed by built areas (UR, n = 31; 43 %), rangeland (RL, n = 3; 4 %), and trees (TR, n = 2; 3 %).

3.4.2. fDOM patterns across LULC types within the optimal scale

Despite the statistically significant explanatory power of the combined LULC and TWI variables for groundwater DOM variability at the 500 m scale, systematic differences among discrete LULC categories were not detected. None of the groundwater DOM metrics (DOC, TPH-like, humic-like, TYR-like fluorescence, FI, β:α, HIX_{corr}, TPH: FA, and SUVA) differed significantly among LULC classes (all $p > 0.08$; Fig. 4). Across LULC categories, several indices, however, showed within-class variability, reflecting heterogeneity in DOM sources and processing independent of the LULC classification. FI varied from <1.2 to >1.8, indicating mixed DOM source contributions; β:α ratios were typically <1, and median HIX_{corr} was >0.5, consistent with processed, humified DOM across all land-use types.

These patterns suggest that, although the 500 m buffer captures a spatial scale relevant to groundwater DOM variability, DOM composition does not reflect a single dominant local land-use signal. Instead, the observed variability likely reflects integrated inputs from mixed land-use types and localised subsurface processing.

3.4.3. Dominant explanatory variables

At 500 m buffer scale, RDA identified surface-water cover as the only LULC variable significantly associated with bulk DOC and fDOM composition (F = 12, p = 0.02; adj. R^2 = 0.11; Fig. 5). TWI also explained a modest but significant portion of DOM variability (F = 4.0, p = 0.03; adj. R^2 = 0.08; Fig. 5). Together, LULC and TWI accounted for 14.2 % of total DOM variation, with unique contributions of 6.4 % (LULC), 3.9 % (TWI), and 3.9 % shared variance (Fig. S2–a). Other LULC classes showed no significant association with DOM composition (all $p \geq 0.4$; adj. $R^2 \leq 0$; Fig. S2–b). These results suggest that the presence of surface water is the most consistently associated LULC-related factor with DOM composition at this spatial scale, while broader LULC types contribute minimally.

3.5. Topographic wetness index and DOM relationships

Groundwater bulk and fDOM exhibited modest but statistically significant associations with topographic wetness across the study region (Fig. 6). DOC was positively correlated with TWI (ρ = 0.33; $p < 0.01$;

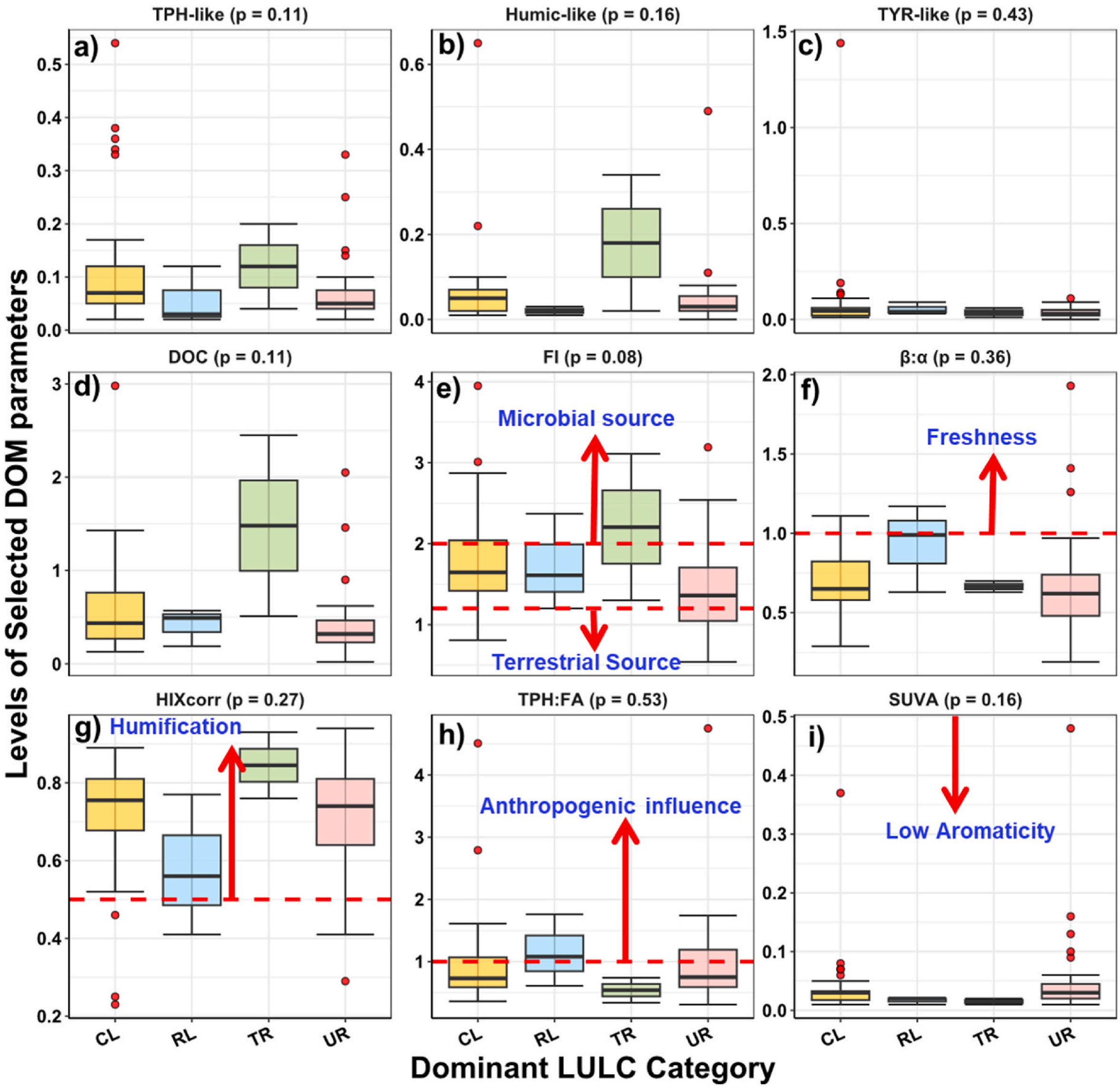

Fig. 4. Boxplots showing the distribution of bulk and fluorescent DOM across groundwater sampling points grouped by dominant land-use/land-cover (LULC) within a 500 m buffer (CL – Cropland ($n = 36$), RL –Rangeland ($n = 3$), TR –Trees ($n = 2$), UR – Built-up ($n = 31$). Parameters include (**a**) tryptophan-like (TPH-like; RU), (**b**) humic-like (RU), (**c**) tyrosine-like (TYR-like; RU), (**d**) dissolved organic carbon (DOC; mg/L), (**e**) fluorescence index (FI), (**f**) β:α ratio, (**g**) humification index (HIX_{corr}), (**h**) tryptophan-to-fulvic ratio (TPH: FA), and (**i**) SUVA ($L.mg^{-1}.m^{-1}$). Boxplots show medians, interquartile ranges, and outliers (red circles). Dashed red lines indicate reference source thresholds for selected parameters (FI at 1.2 and 2.0 (Cory and McKnight, 2005); β:α at 1.0 (Huguet et al., 2009); HIX-corr at 0.5 (Ohno, 2002); and TPH: FA at 1.0 (Baker, 2001, 2002)). Red arrows show whether samples lie above or below the reference thresholds. Statistical significance was evaluated using the Kruskal-Wallis test. (For interpretation of the references to colour in this figure legend, the reader is referred to the Web version of this article.)

Fig. 6a). Fluorescent DOM components also showed consistent positive associations, including humic-like ($\rho = 0.26, p < 0.05$; Fig. 6b), TPH-like ($\rho = 0.30, p = 0.01$; Fig. 6c), and fulvic-like fractions ($\rho = 0.32, p < 0.01$; Fig. 6d).

Generalised linear models fitted across all samples further indicated positive linear relationships between TWI and both bulk and fluorescent DOM, although only a modest proportion of the observed variability was explained, consistent with multiple interacting controls on DOM composition, including aquifer heterogeneity, groundwater residence time, redox conditions, contamination sources, well depth, and water-source type. DOC increased significantly with TWI (slope coefficient $\beta = 0.35$, 95 % CI 0.13 – 0.58, $p = < 0.01$; Adj. $R^2 = 12$ %), while humic-like ($\beta = 0.06$, 95 % CI 0.02 – 0.11, $p = 0.01$; Adj. $R^2 = 9$ %), TPH-like ($\beta = 0.06$, 95 % CI 0.02 – 0.11, $p = 0.01$; Adj. $R^2 = 9$ %), and fulvic-like DOM components ($\beta = 0.11$, 95 % CI 0.02 – 0.21, $p = 0.03$; Adj. $R^2 = 7$ %) showed similarly modest but significant responses. These results suggest that hydrological convergence is consistent with enhanced DOM mobilisation in groundwater, but the strength of this influence varies among DOM fractions.

3.6. Co-variation of nitrate/chloride and sulphate/chloride ratios with DOM variables

Nitrate enrichment in groundwater showed modest correlations with DOM composition (Fig. 7; Fig. S5). NO_3^-/Cl^- co-varied with SO_4^{2-}/Cl^- (Spearman $\rho = 0.43$, $p < 0.05$; Fig. 7a), suggesting shared input mechanism for nitrate and sulphate, potentially linked to fertilisers and mixed wastewater inputs. NO_3^-/Cl^- was not significantly correlated with humic-like fluorescence, consistent with humic-like DOM reflecting older, more processed and variably sourced organic matter that is not associated with recent nitrate inputs. In contrast, NO_3^-/Cl showed a weak negative correlation with fulvic-like components ($\rho = -0.30$,

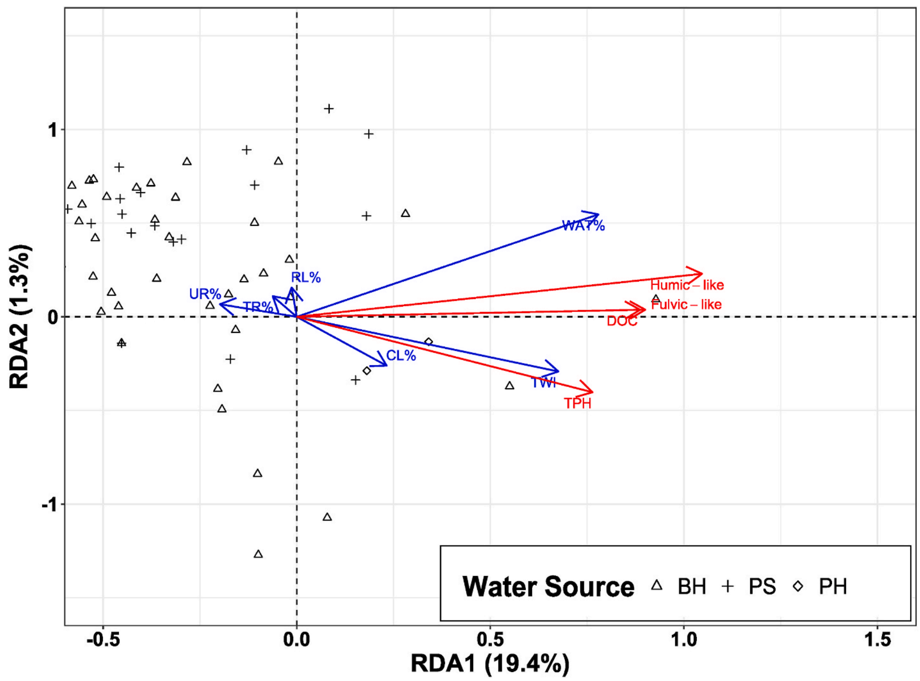

Fig. 5. RDA biplot on the 500 m buffer analysis showing the influence of each land-use/land-cover (LULC) class on the groundwater DOM variables (dissolved organic carbon [DOC], Humic-like, Fulvic-like and Tryptophan-like [TPH-like] fluorescence) and topographic wetness index (TWI) across different water sources. Blue arrows represent Hellinger-transformed land use predictors (WAT% for surface water cover, CL% for cropland, UR% for built-up areas, %RL for rangeland, and TR% for tree cover) and TWI, while red arrows indicate response variables. Sampling points are shaped by water source: boreholes (BH), protected springs (PS), and piped groundwater systems (PH). Axis labels indicate the percentage of constrained variance explained by each axis. (For interpretation of the references to colour in this figure legend, the reader is referred to the Web version of this article.)

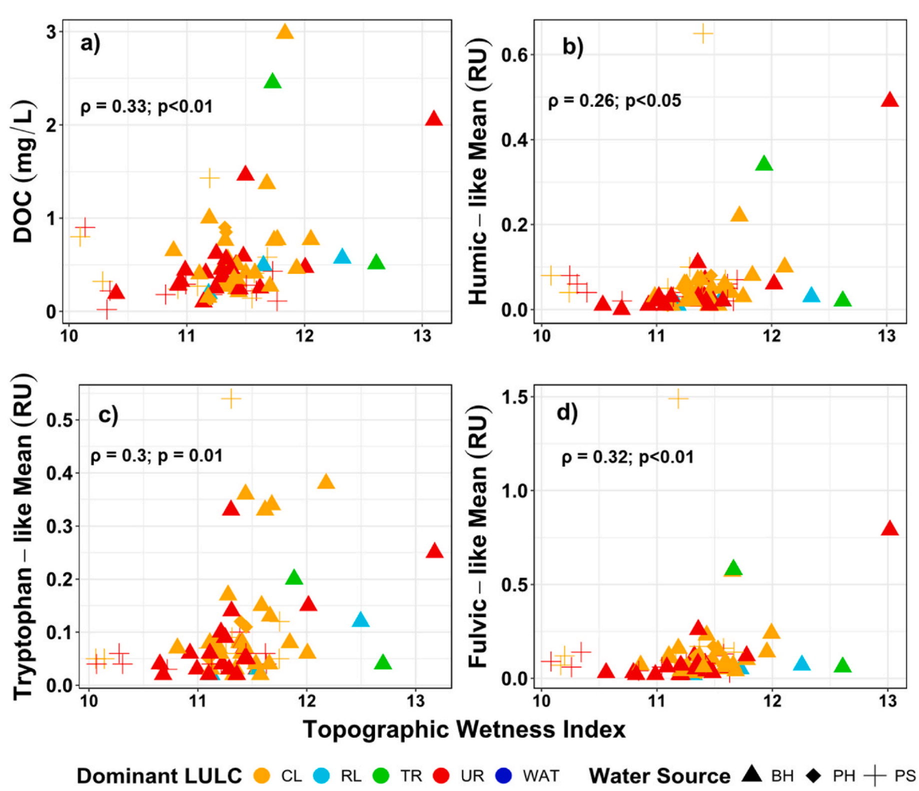

Fig. 6. Relationships between topographic wetness index (TWI) and fluorescent and bulk dissolved organic matter (DOM) components. Panels show (**a**) dissolved organic carbon (DOC, mg/L), (**b**) humic-like DOM (RU), (**c**) tryptophan-like DOM (RU), and (**d**) fulvic-like DOM (RU). Points are coloured by dominant land-use/land-cover (LULC: TR = Trees, UR = Urban, RL = Rangeland, CL = Cropland) and shaped by water source (BH = Borehole, PS = Protected Spring, PH =Piped groundwater system). Annotated values are Spearman's rank correlation coefficient (ρ) and associated *p*-values; all groundwater samples (*n* = 72) considered.

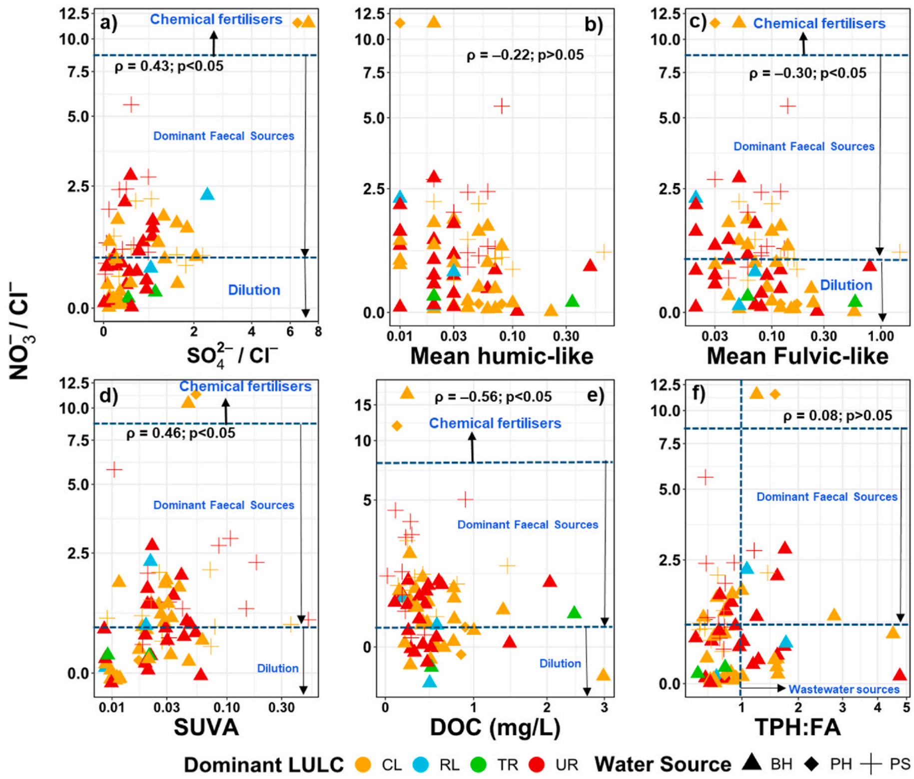

Fig. 7. Relationships between NO_3^-/Cl^- molar ratios and fDOM, bulk DOC and geochemical indicators across sampling sites. Points are coloured by dominant LULC type (CL- Cropland, RL- Rangeland, WAT – Water, TR – Trees, UR – built-up), and shaped by water source (BH – Boreholes, PH – Piped groundwater system, PS – Protected springs). Each panel shows a specific indicator: **(a)** SO_4^{2-}/Cl^-, **(b)** Humic-like mean (RU), **(c)** Fulvic-like fluorescence (RU), **(d)** SUVA (L. $mg^{-1}.m^{-1}$), **(e)** DOC (mg/L), and **(f)** Tryptophan: fulvic acid (TPH: FA). Dashed horizontal lines indicate the conceptual NO_3^-/Cl^- ratio thresholds used to infer the potential nitrate sources (ARGOSS, 2001), together with Spearman's rank correlation coefficients (ρ), and their statistical significance (assessed at $p < 0.05$). Black arrows show whether samples lie above or below the reference thresholds. Axes are displayed using log or pseudo-log transformations as appropriate.

$p < 0.05$; Fig. 7b and c), suggesting a relative reduction of fulvic fractions in nitrate-rich waters. Both NO_3^-/Cl^- and SO_4^{2-}/Cl^- were positively correlated with SUVA (ρ = 0.43 and 0.27, respectively; $p < 0.05$; Fig. 7d), despite uniformly low absolute SUVA values (0 – 0.5), indicating a slight relative shift towards more aromatic DOM. NO_3^-/Cl^- correlated moderately with DOC (ρ = −0.56, $p < 0.05$; Fig. 7e), with higher DOC generally associated with lower nitrate enrichment, consistent with potential attenuation in organic-rich groundwater. Conversely, NO_3^-/Cl^- was not significantly correlated with TPH: FA (Fig. 7f), with wastewater-associated DOM signals variably expressed across both low and high nitrate enrichment, indicating that direct organic waste inputs were not consistently associated with the NO_3^-/Cl^- tracers.

Notably, consistent with ARGOSS (2001), most samples across all LULC types fell within the NO_3^-/Cl^- range (1:1 – 8:1) typically associated with faecal-derived nitrogen sources. This pattern is suggestive of contributions from on-site sanitation and animal waste to groundwater nitrate (ARGOSS, 2001). Some samples, mainly associated with cropland, exhibited higher NO_3^-/Cl^- ratios that are consistent with nitrate derived from inorganic fertilisers. However, the substantial overlap among land-use types indicates that mixed-source regimes are likely, reflecting the influence of multiple anthropogenic nitrogen inputs, as observed in groundwater systems elsewhere (Boumaiza et al., 2026; Sacchi et al., 2013).

4. Discussion

4.1. *DOM composition indicates processed fractions from mixed terrestrial and microbial sources*

Groundwater DOM across eastern and central Uganda was dominated by weakly aromatic material, with humic fraction contributing only ~17 % of total fluorescence yet showing relatively high humification (SUVA <0.5 L $mg^{-1}.m^{-1}$; median $HIX_{corr} > 0.5$; $\beta:\alpha < 1$). The combination of low SUVA with high HIX_{corr} suggests a pool of relatively processed organic matter with preserved humified fluorescence, consistent with extensive oxidative reworking of organic matter that depletes aromatic rings (D'Andrilli et al., 2022; Hansen et al., 2016). The FI (median ~ 1.6) points to mixed terrestrial and microbial contributions, reflecting both surface-derived inputs and *in-situ* microbial transformation. Such compositional signatures are consistent with the recent reports of microbially derived DOM in Gulu groundwater (Wilson et al., 2024b), and are comparable with patterns across diverse tropical environments, including pre-monsoon groundwater in Patna, India (Wilson et al., 2023), Holocene aquifers in Cambodia (Richards et al., 2019), and groundwater-fed streams in Costa Rican rainforests (Osburn et al., 2018).

4.2. *Hydrological connectivity is associated with groundwater DOM composition*

Contrary to the hypothesis that land-use would primarily shape groundwater DOM composition, our results show no significant LULC-related differences at the spatial scales tested (Fig. 4). Instead, modest but statistically significant relationships (adj. $R^2 \sim 0.14$; Fig. 5) were identified between groundwater DOM and both TWI and surface-water cover within a 500 m buffer. Whilst these modest relationships reflect the influence of multiple controlling factors on DOM composition (*e.g.,* aquifer lithology, groundwater residence time, redox conditions, recharge pathways, well construction, and local contamination sources), they point to a consistent role of terrain-mediated flow accumulation in influencing the observed DOM variability.

Sites with higher TWI, indicative of greater potential for lateral flow convergence and near-surface saturation (Beven and Kirkby, 1979), were generally associated with modest increases in bulk and fluorescent DOM across the study region (Fig. 6). These patterns suggest that groundwater DOM in this region is less strongly associated with local vertical transport beneath individual land parcels and instead more consistent with potential lateral redistribution and mobilisation of organic matter along hydrologically convergent zones. The relatively weak LULC signal therefore likely reflects the influence of upslope contributions integrated through surface–subsurface connectivity, rather than the influence of land cover immediately surrounding sampling points.

Potential buffer methodological artefacts were considered as a source of the muted LULC–DOM relationships. Circular buffers can introduce focal-area bias (FAB), whereby peripheral areas disproportionately influence aggregated land-cover metrics (Huck et al., 2025). However, correcting LULC metrics for FAB produced only a marginal improvement in model performance at 500 m scale (adj. R^2 increasing from 14.2 % to 14.6 %). Moreover, the general consistency of results across multiple buffer sizes tested suggests that geometric bias alone cannot explain the observed patterns. This observation likely reflects the fact that LULC influences on groundwater DOM are not strictly tied to geometric distances, due to high heterogeneity in both surface conditions and groundwater chemistry. These findings align with studies that demonstrate substantial lateral fluxes of organic matter from riparian and hyporheic zones into groundwaters (Lapworth et al., 2009), and with regional evidence for dynamic groundwater–surface water exchange within the Kyoga and Victoria basins (Kayendeke and French, 2019; Owor et al., 2011).Whilst the absence of hydraulic gradient and temporal data limits our ability to distinguish between enhanced recharge, lateral redistribution, or shared topographic controls, the observed associations are consistent with increased surface–subsurface interactions in hydrologically convergent landscape positions.

4.3. Surface waters and near-surface zones as potential DOM reservoirs for aquifers

Surface waters showed strong enrichment in bulk DOC and all fDOM components compared with groundwater, yet several optical fingerprints were largely similar (Fig. 3). This compositional similarity suggests partial preservation of surface-derived DOM signatures in groundwater and is consistent with potential surface water-groundwater interactions within the hyporheic zone and broader near-surface environment (Lapworth et al., 2009). Groundwater sites with surface water within a 500 m radius (hereafter "proximal sites") exhibited relatively higher bulk DOC, humic-like, and TPH-like DOM than sites lacking surface water in the same radius, although these differences were not statistically significant (Fig. S3). Across water types, however, bulk DOC and fDOM levels at proximal sites overlapped with those observed in surface waters, whereas significant differences were apparent between surface waters and groundwater sites without surface water in the radius (Fig. S3). Most compositional indices did not differ significantly among the water groups, further indicating limited compositional differentiation despite differences in DOM levels.

Although the sampled surface waters were drawn mainly from the Nile River and Lake Victoria and may not be directly connected to all sampled wells, they represent plausible regional surface water DOM endmembers against which groundwater DOM characteristics can be compared. Therefore, the observed compositional overlap between surface waters and groundwater suggests that surface waters and associated near-surface zones may function as transient reservoirs of organic matter that could contribute to groundwater where hydrological connectivity exists through hyporheic, parafluvial, or paralacustrine exchange processes (Findlay, 1995; Lapworth et al., 2009), although direct evidence of hydraulic connectivity was not assessed in this study.

Moreover, the positive association between groundwater bulk and fDOM and hydrological convergence (Spearman, $\rho \geq 0.3$; $p \leq 0.01$) further suggests that terrain-driven accumulation zones may facilitate an increased likelihood of surface–subsurface connectivity. These zones are prone to episodic near-surface saturation and focused recharge, conditions under which organic matter from surface waters or near-surface zones, such as shallow soils or hyporheic regions, can be mobilised into the subsurface. Surface–subsurface transition zones are widely recognised as active biogeochemical interfaces where organic matter undergoes partial transformation (Lapworth et al., 2009; Lynch et al., 2019; Stegen et al., 2016). The persistence of surface-like optical signals in groundwater is therefore consistent with contributions from surface-associated DOM, or DOM processed under comparable conditions, particularly within the hyporheic zone.

4.4. Anthropogenic nitrogen alters DOM fate rather than supply

Most groundwater samples clustered within NO_3^-/Cl^- ratios consistent with those commonly associated with faecal-derived nitrogen sources (ARGOSS, 2001, Fig. 7). Given the widespread usage of pit latrines and incidences of open defecation across the study region (UBOS, 2024), these ratios are consistent with regionally diffuse anthropogenic nitrate inputs that are mobilised independently of bulk organic carbon transport. The co-variation of NO_3^-/Cl^- with SO_4^{2-}/Cl^-, together with the absence of significant relationships with protein-like fluorescence or the TPH:FA ratio, further indicates that nitrate inputs are not directly linked to the co-delivery of labile organic matter. Although some samples showed high TPH:FA ratios (>1; Fig. 7), this overall pattern suggests that nitrate in the aquifers primarily originates from oxidised anthropogenic nitrogen sources, including microbially transformed faecal nitrogen and fertiliser-derived nitrate, rather than fresh sewage-derived inputs.

Notably, higher NO_3^-/Cl^- ratios were associated with lower DOC concentrations ($\rho = -0.56$, $p < 0.05$) and a relative increase in SUVA ($\rho = 0.43$; $p < 0.05$), consistent with preferential loss of labile DOM (bioavailable and microbially reactive DOM fractions) and enrichment of more humic residual fractions within an overall weakly aromatic DOM pool. Such behaviour is consistent with nitrate-stimulated microbial oxidation of organic carbon, in which nitrate acts as an alternative electron acceptor (Bulseco et al., 2019; Rivett et al., 2008; Song et al., 2020). These results suggest that, in these aquifers, anthropogenic nitrate plausibly modifies the fate of groundwater DOM through enhanced carbon processing, rather than acting as a direct source of organic matter (Taylor and Townsend, 2010). This interpretation is further supported by redox conditions, as *Eh* was negatively correlated with DOC ($\rho = -0.39$; $p < 0.05$) and positively correlated with NO_3^-/Cl^- ($\rho = 0.45$; $p < 0.05$; Fig. S5), consistent with more oxidising, nitrate-enriched groundwater associated with lower DOC.

5. Conclusions

This study quantified humic-like and protein-like fractions of groundwater DOM and examined their relationships with LULC, hydrological convergence (quantified by TWI) and anthropogenic tracers (NO_3^-/Cl^-, SO_4^{2-}/Cl^-) across the Kyoga and Victoria basins in eastern and central Uganda. Groundwater DOM was dominated by weakly aromatic, relatively processed material with mixed terrestrial and microbial origins (SUVA <0.5 L $mg^{-1}.m^{-1}$; median $HIX_{corr} > 0.5$, $\beta:\alpha < 1$, and FI $\sim$ 1.6), consistent with extensive subsurface transformation and diffuse organic inputs. This study provides evidence on groundwater carbon dynamics in a data-scarce region of East Africa, whilst introducing new interpretative approaches for associations between land-use, hydrology, and groundwater DOM.

Surface-water cover showed a consistent significant association with groundwater DOM, whilst other LULC classes exhibited weak or non-significant relationships, even at the spatial scale of maximum explanatory power (viz. 500 m). In contrast, hydrological convergence explained a modest but consistent fraction of variation in bulk DOC and selected fDOM components, suggesting a potential role of terrain-driven lateral accumulation in redistributing organic matter towards aquifer recharge zones. These findings identify TWI as a useful explanatory metric for groundwater DOM variability in this and potentially other tropical and sub-tropical regions with comparable hydroclimatic and geomorphological conditions.

Nitrate enrichment was associated with shifts in DOM composition, consistent with preferential loss of labile fractions and a shift towards more processed DOM within an otherwise weakly aromatic pool, plausibly reflecting enhanced subsurface carbon processing in nitrate-impacted groundwater.

Overall, groundwater DOM in this region is more significantly associated with hydrological setting and indicators of anthropogenic influence than with individual land-use classes. Surface waters and near-surface zones are likely dynamic reservoirs and transformation environments for DOM entering aquifers. Broadly, these results suggest three implications: 1) aquifer carbon pools in the region are likely sensitive to factors that induce changes in hydrological connectivity; 2) safeguarding groundwater quality in the region may require protecting riparian zones and surface-water integrity, in addition to managing the broad land-use categories; and 3) nitrate-associated DOM shifts, potentially linked to carbon cycling, may be more widespread in tropical groundwaters than currently recognised.

Future work combining detailed hydrogeological and lithological characterisation with isotopic and DOM-tracer analyses will be important for resolving DOM and nitrate sources, including potential lithological controls, groundwater evolution, and assessing temporal variability associated with functional (*e.g.*, rainfall-driven) connectivity.

CRediT authorship contribution statement

Derick Muloogi: Conceptualization, Data curation, Formal analysis, Investigation, Methodology, Visualization, Writing – original draft. **Daren C. Gooddy:** Methodology, Writing – review & editing. **David A. Polya:** Conceptualization, Funding acquisition, Methodology, Supervision, Writing – review & editing. **Laura A. Richards:** Conceptualization, Funding acquisition, Investigation, Methodology, Project administration, Resources, Supervision, Writing – review & editing.

Declaration of competing interest

The authors declare that they have no known competing financial interests or personal relationships that could have appeared to influence the work reported in this paper.

Acknowledgements

We gratefully acknowledge the support from The University of Manchester FSE Dean's Doctoral Scholarship (to DM), a Dame Kathleen Ollerenshaw Fellowship (to LAR), a UKRI Future Leaders Fellowship (MR/Y016327/1 to LAR et al.; www.aquaroad.org), and the International Science Partnership Fund (ISPF) – England Project (ODA; 2023 – 2024) through the University of Manchester (to LAR et al.). We are thankful to the Ministry of Water and Environment, Uganda, particularly Caroline Wafula, Abudallah Matovu, and Alex Kyombo, the Jinja District Water Officer, for granting permissions to access community water points during our sampling campaign. We also appreciate the valuable support from George JL Wilson, Farah A. Tasneem, and Yasin Koire during fieldwork. Peter Williams is appreciated for facilitating the EEM analysis at BGS, Wallingford, UK. We also thank Jordan Gaskell and Rosie Byrne at the University of Manchester for their analytical support through MAGU. Jonny Huck, Kirsty Watkinson and Darren Reynolds are thanked for discussions. We acknowledge two anonymous reviewers for their constructive comments. The views expressed here do not necessarily reflect those of the institutions, funders, or individuals acknowledged.

Appendix A. Supplementary data

Supplementary data to this article can be found online at https://doi.org/10.1016/j.apgeochem.2026.106955.

Data availability

Data supporting this study are provided in the manuscript and accompanying Supplementary Information.

References

Aiken, G.R., Hsu-Kim, H., Ryan, J.N., 2011. Influence of dissolved organic matter on the environmental fate of metals, nanoparticles, and colloids. https://doi.org/10.1021/es103992s.

ARGOSS, 2001. Guidelines for assessing the risk to groundwater from on-site sanitation. British Geological Survey Commissioned Report, CR/01/142, p. 97.

Baker, A., 2001. Fluorescence excitation− emission matrix characterization of some sewage-impacted rivers. Environ. Sci. Technol. 35, 948–953. https://doi.org/10.1021/es000177t.

Baker, A., 2002. Fluorescence properties of some farm wastes: implications for water quality monitoring. Water Res. 36, 189–195. https://doi.org/10.1016/S0043-1354(01)00210-X.

Baker, A., Curry, M., 2004. Fluorescence of leachates from three contrasting landfills. Water Res. 38, 2605–2613. https://doi.org/10.1016/j.watres.2004.02.027.

Baker, A., Lamont-Biack, J., 2001. Fluorescence of dissolved organic matter as a natural tracer of ground water. Groundwater 39, 745–750. https://doi.org/10.1111/j.1745-6584.2001.tb02365.x.

Balasubramaniyan, G., Ganesan, D.A., Murugesan, B., Swaminathan, B., Karuppannan, S., Duraisamy, K., 2025. AHP and Geospatial technology-based assessment of groundwater potential zones in Natham taluk, Tamil nadu, India. Sci. Rep. 15, 28045. https://doi.org/10.1038/s41598-025-13829-z.

Beven, K.J., Kirkby, M.J., 1979. A physically based, variable contributing area model of basin hydrology/Un modèle à base physique de zone d'appel variable de l'hydrologie du bassin versant. Hydrol. Sci. Bull. 24, 43–69. https://doi.org/10.1080/02626667909491834.

BGS, 2019. Africa Groundwater Atlas Country Hydrogeology Maps. British Geological Survey Open Report. https://www.bgs.ac.uk/geology-projects/africa-groundwater-atlas/.

Boumaiza, L., Ammar, S.B., Chesnaux, R., Mayer, B., Sacchi, E., Huneau, F., Garel, É., Johannesson, K.H., Stotler, R.L., Khouatmia, M., Nlend, B., Knöller, K., Stumpp, C., 2026. An isotope mixing-based clustering approach for an improved apportionment of nitrate sources in groundwater systems. Sci. Total Environ. 1010, 181158. https://doi.org/10.1016/j.scitotenv.2025.181158.

Bracken, L.J., Wainwright, J., Ali, G.A., Tetzlaff, D., Smith, M.W., Reaney, S.M., Roy, A. G., 2013. Concepts of hydrological connectivity: research approaches, pathways and future agendas. Earth Sci. Rev. 119, 17–34. https://doi.org/10.1016/j.earscirev.2013.02.001.

Bulseco, A.N., Giblin, A.E., Tucker, J., Murphy, A.E., Sanderman, J., Hiller-Bittrolff, K., Bowen, J.L., 2019. Nitrate addition stimulates microbial decomposition of organic matter in salt marsh sediments. Glob. Change Biol. 25, 3224–3241. https://doi.org/10.1111/gcb.14726.

Burt, T., Pinay, G., 2005. Linking hydrology and biogeochemistry in complex landscapes. Prog. Phys. Geogr. 29, 297–316. https://doi.org/10.1191/0309133305pp450ra.

Catipovic, L., Tzortziou, M., Turner, K.J., Harringmeyer, J., Goes, J., Gomes, H., Wu, J., O'Shea, R.E., Guild, L.S., Kalyan, B., 2026. Dissolved organic matter dynamics in South African nearshore waters and freshwater systems: linkages to changing human activity, episodic events, and biodiversity. J. Geophys. Res. Biogeosci. 131. https://doi.org/10.1029/2025JG009331.

Chen, M., Price, R.M., Yamashita, Y., Jaffé, R., 2010. Comparative study of dissolved organic matter from groundwater and surface water in the Florida coastal everglades using multi-dimensional spectrofluorometry combined with multivariate statistics. Appl. Geochem. 25, 872–880. https://doi.org/10.1016/j.apgeochem.2010.03.005.

Chin, Y.-Ping, Aiken, George, O'Loughlin, Edward, 1994. Molecular weight, polydispersity, and spectroscopic properties of aquatic humic substances. Environ. Sci. Technol. 28, 1853–1858. https://doi.org/10.1021/es00060a015.

Coble, P.G., 1996. Characterization of marine and terrestrial DOM in seawater using excitation-emission matrix spectroscopy. Mar. Chem. 51, 325–346. https://doi.org/10.1016/0304-4203(95)00062-3.

Cory, R.M., McKnight, D.M., 2005. Fluorescence spectroscopy reveals ubiquitous presence of oxidized and reduced quinones in dissolved organic matter. Environ. Sci. Technol. 39, 8142–8149. https://doi.org/10.1021/es0506962.

D'Andrilli, J., Silverman, V., Buckley, S., Rosario-Ortiz, F.L., 2022. Inferring ecosystem function from dissolved organic matter optical properties: a critical review. Environ. Sci. Technol. 56, 11146–11161. https://doi.org/10.1021/acs.est.2c04240.

Dwivedi, D., Poeppl, R.E., Wohl, E., 2025. Hydrological connectivity: a review and emerging strategies for integrating measurement, modeling, and management. Front. Water 7, 1496199. https://doi.org/10.3389/frwa.2025.1496199.

DWRM, 2014. Uganda Catchment Management Planning Guidelines. https://weadapt.org/wp-content/uploads/2024/03/uganda_cmp_guidelines.pdf.

Epting, S.M., Hosen, J.D., Alexander, L.C., Lang, M.W., Armstrong, A.W., Palmer, M.A., 2018. Landscape metrics as predictors of hydrologic connectivity between Coastal Plain forested wetlands and streams. Hydrol. Process. 32, 516–532. https://doi.org/10.1002/hyp.11433.

Esri, 2023. Esri Land Cover [A 10-meter annual map of Earth's land surface from 2017-2024]. Arcgis Living Atlas of the World. https://livingatlas.arcgis.com/landcover/.

Fellman, J.B., Hood, E., Spencer, R.G., 2010. Fluorescence spectroscopy opens new windows into dissolved organic matter dynamics in freshwater ecosystems: a review. Limnol. Oceanogr. 55, 2452–2462. https://doi.org/10.4319/lo.2010.55.6.2452.

Findlay, S., 1995. Importance of surface-subsurface exchange in stream ecosystems: the hyporheic zone. Limnol. Oceanogr. 40, 159–164. https://doi.org/10.4319/lo.1995.40.1.0159.

Findlay, S., Sinsabaugh, R.L., 2003. Aquatic Ecosystems: Interactivity of Dissolved Organic Matter. Academic press.

Forest Trends, 2024. Illegal Deforestation and Agricultural Commodities: Uganda. https://www.forest-trends.org/wp-content/uploads/2024/08/FRC-Dashboard_Uganda_Final.pdf.

Gabor, R.S., Baker, A., McKnight, D.M., Miller, M.P., 2014. Fluorescence Indices and their Interpretation. Cambridge University Press, Cambridge, UK.

Gad, M., Khomami, N.T.S., Krieg, R., Schor, J., Philippe, A., Lechtenfeld, O.J., 2024. Environmental Drivers of Dissolved Organic Matter Composition across Central European Aquatic Systems: a novel correlation-based machine learning and FT-ICR MS approach. Water Res., 123018 https://doi.org/10.1016/j.watres.2024.123018.

GFW, 2024. Uganda Deforestation Rates & Statistics. https://www.globalforestwatch.org/dashboards/country/UGA/.

Hansen, A.M., Kraus, T.E., Pellerin, B.A., Fleck, J.A., Downing, B.D., Bergamaschi, B.A., 2016. Optical properties of dissolved organic matter (DOM): effects of biological and photolytic degradation. Limnol. Oceanogr. 61, 1015–1032. https://doi.org/10.1002/lno.10270.

Harjung, A., Schweichhart, J., Rasch, G., Griebler, C., 2023. Large-scale study on groundwater dissolved organic matter reveals a strong heterogeneity and a complex microbial footprint. Sci. Total Environ. 854, 158542. https://doi.org/10.1016/j.scitotenv.2022.158542.

Hosen, J.D., McDonough, O.T., Febria, C.M., Palmer, M.A., 2014. Dissolved organic matter quality and bioavailability changes across an urbanization gradient in headwater streams. Environ. Sci. Technol. 48, 7817–7824. https://doi.org/10.1021/es501422z.

Howard, K.W.F., Karundu, J., 1992. Constraints on the exploitation of basement aquifers in East Africa — water balance implications and the role of the regolith. J. Hydrol. 139, 183–196. https://doi.org/10.1016/0022-1694(92)90201-6.

Huck, J.J., Dennis, M., Labib, S.M., 2025. Addressing bias in the use of buffers for focal and geographically weighted analyses. Int. J. Geogr. Inf. Sci. 39, 1183–1202. https://doi.org/10.1080/13658816.2024.2440048.

Huguet, A., Vacher, L., Relexans, S., Saubusse, S., Froidefond, J.-M., Parlanti, E., 2009. Properties of fluorescent dissolved organic matter in the Gironde Estuary. Org. Geochem. 40, 706–719. https://doi.org/10.1016/j.orggeochem.2009.03.002.

ICPAC, 2017. Africa - Admin Level 0. https://geoportal.icpac.net/layers/geonode%3Aafr_g2014_2013_0.

IFDC, A.F.A.P., 2018. Assessment of fertilizer distribution systems and opportunities for developing fertilizer blends in Uganda. https://agra.org/wp-content/uploads/2020/08/Uganda-Report_Assessment-of-Fertilizer-Distribution-Systems-and-Opportunities-for-Developing-Fertilizer-Blends.pdf.

Jancewicz, K., Migoń, P., Kasprzak, M., 2019. Connectivity patterns in contrasting types of tableland sandstone relief revealed by Topographic Wetness Index. Sci. Total Environ. 656, 1046–1062. https://doi.org/10.1016/j.scitotenv.2018.11.467.

Kayendeke, E.J., French, H.K., 2019. Characterising the hydrological regime of a tropical papyrus wetland in the Lake Kyoga Basin, Uganda. In: Bamutaze, Y., Kyamanywa, S., Singh, B.R., Nabanoga, G., Lal, R. (Eds.), Agriculture and Ecosystem Resilience in Sub Saharan Africa: Livelihood Pathways Under Changing Climate. Springer International Publishing, Cham, pp. 213–236. https://doi.org/10.1007/978-3-030-12974-3_10.

Kopecký, M., Macek, M., Wild, J., 2021. Topographic Wetness Index calculation guidelines based on measured soil moisture and plant species composition. Sci. Total Environ. 757, 143785. https://doi.org/10.1016/j.scitotenv.2020.143785.

Lang, M., McCarty, G., Oesterling, R., Yeo, I.-Y., 2013. Topographic metrics for improved mapping of forested wetlands. Wetlands 33, 141–155. https://doi.org/10.1007/s13157-012-0359-8.

Lapworth, D., Gooddy, D., Allen, D., Old, G., 2009. Understanding groundwater, surface water, and hyporheic zone biogeochemical processes in a Chalk catchment using fluorescence properties of dissolved and colloidal organic matter. J. Geophys. Res. Biogeosci. 114. https://doi.org/10.1029/2009JG000921.

Lapworth, D.J., Gooddy, D., Butcher, A., Morris, B., 2008. Tracing groundwater flow and sources of organic carbon in sandstone aquifers using fluorescence properties of dissolved organic matter (DOM). Appl. Geochem. 23, 3384–3390.

Lapworth, D.J., Kinniburgh, D.G., 2009. An R script for visualising and analysing fluorescence excitation–emission matrices (EEMs). Comput. Geosci. 35, 2160–2163. https://doi.org/10.1016/j.cageo.2008.10.013.

Lawson, M., Polya, D.A., Boyce, A.J., Bryant, C., Mondal, D., Shantz, A., Ballentine, C.J., 2013. Pond-derived organic carbon driving changes in arsenic hazard found in asian groundwaters. Environ. Sci. Technol. 47, 7085–7094. https://doi.org/10.1021/es400114q.

Legendre, P., Gallagher, E.D., 2001. Ecologically meaningful transformations for ordination of species data. Oecologia 129, 271–280. https://doi.org/10.1007/s004420100716.

Lindsay, J.B., 2016. Whitebox GAT: a case study in geomorphometric analysis. Comput. Geosci. 95, 75–84. https://doi.org/10.1016/j.cageo.2016.07.003.

Lynch, L.M., Sutfin, N.A., Fegel, T.S., Boot, C.M., Covino, T.P., Wallenstein, M.D., 2019. River channel connectivity shifts metabolite composition and dissolved organic matter chemistry. Nat. Commun. 10, 459. https://doi.org/10.1038/s41467-019-08406-8.

Lyons, M., Ingham, K., Kiwanuka, M.M.S., 2025. Land of Uganda. Encyclopaedia Britannica. https://www.britannica.com/place/Uganda/Land.

MAAIF, 2016. NATIONAL FERTILISER POLICY.

Manly, B.F., 2018. Randomization, Bootstrap and Monte Carlo Methods in Biology. chapman and hall/CRC. https://doi.org/10.1201/9781315273075.

McDonough, L.K., Andersen, M.S., Behnke, M.I., Rutlidge, H., Oudone, P., Meredith, K., O'Carroll, D.M., Santos, I.R., Marjo, C.E., Spencer, R.G., 2022. A new conceptual framework for the transformation of groundwater dissolved organic matter. Nat. Commun. 13, 2153. https://doi.org/10.1038/s41467-022-29711-9.

McKnight, D.M., Boyer, E.W., Westerhoff, P.K., Doran, P.T., Kulbe, T., Andersen, D.T., 2001. Spectrofluorometric characterization of dissolved organic matter for indication of precursor organic material and aromaticity. Limnol. Oceanogr. 46, 38–48.

Moore, O.C., Holt, A.D., Richards, L.A., McKenna, A.M., Spencer, R.G., Lapworth, D.J., Polya, D.A., Lloyd, J.R., van Dongen, B.E., 2024. Characterisation of dissolved organic matter in two contrasting arsenic-prone sites in Kandal Province, Cambodia. Org. Geochem. 198, 104886. https://doi.org/10.1016/j.orggeochem.2024.104886.

Muloogi, D., Wilson, G.J.L., Ahmed, F.T., Polya, D.A., Richards, L.A., 2025. Groundwater chemistry of contrasting hydrogeological settings in Uganda. Presented at EGU General Assembly 2025. https://doi.org/10.5194/egusphere-egu25-662 (EGU25-662).

Muloogi, D., Wilson, G.J.L., Ahmed, F.T., Polya, D.A., Richards, L.A., 2026. Spatial variations in groundwater chemistry in Uganda: geogenic origins and geochemical controls across diverse hydrogeological settings. Appl. Geochem., 106738 https://doi.org/10.1016/j.apgeochem.2026.106738.

Murphy, K.R., Stedmon, C.A., Graeber, D., Bro, R., 2013. Fluorescence spectroscopy and multi-way techniques. In: PARAFAC. Analytical methods, 5, pp. 6557–6566. https://doi.org/10.1039/C3AY41160E.

MWE, 2025. Uganda water supply Atlas. http://wsdb.mwe.go.ug/index.php/reports/national.

Namaalwa, S., van Dam, A.A., Gettel, G.M., Kaggwa, R.C., Zsuffa, I., Irvine, K., 2020. The impact of wastewater discharge and agriculture on water quality and nutrient retention of Namatala wetland, Eastern Uganda. Front. Environ. Sci. 8. https://doi.org/10.3389/fenvs.2020.00148, 2020.

NEMA, 2016. State of the Environment Report for Uganda 2014. National Environment Management Authority (NEMA), Kampala.

Neumann, R.B., Ashfaque, K.N., Badruzzaman, A., Ashraf Ali, M., Shoemaker, J.K., Harvey, C.F., 2010. Anthropogenic influences on groundwater arsenic concentrations in Bangladesh. Nat. Geosci. 3, 46–52. https://doi.org/10.1038/ngeo685.

Nsubuga, F.N., Namutebi, E.N., Nsubuga-Ssenfuma, M., 2014. Water resources of Uganda: an assessment and review. https://doi.org/10.4236/jwarp.2014.614120.

Nyenje, P., Foppen, J., Uhlenbrook, S., Lutterodt, G., 2014. Using hydrochemical tracers to assess impacts of unsewered urban catchments on hydrochemistry and nutrients in groundwater. Hydrol. Process. 28, 5860–5878. https://doi.org/10.1002/hyp.10070.

Nyenje, P.M., Foppen, J.W., Kulabako, R., Muwanga, A., Uhlenbrook, S., 2013. Nutrient pollution in shallow aquifers underlying pit latrines and domestic solid waste dumps in urban slums. J. Environ. Manag. 122, 15–24. https://doi.org/10.1016/j.jenvman.2013.02.040.

Obu, J., Lantuit, H., Myers-Smith, I., Heim, B., Wolter, J., Fritz, M., 2017. Effect of terrain characteristics on soil organic carbon and total nitrogen stocks in soils of Herschel Island, Western Canadian Arctic. Permafr. Periglac. Process. 28, 92–107. https://doi.org/10.1002/ppp.1881.

Obubu, J.P., Mengistou, S., Odong, R., Fetahi, T., Alamirew, T., 2022. Determination of the connectedness of land use, land cover change to water quality status of a shallow Lake: a case of Lake Kyoga Basin, Uganda. Sustainability 14. https://doi.org/10.3390/su14010372.

OCHA, 2020. Uganda - subnational administrative boundaries||sourced from Uganda bureau of statistics with support from WHO. https://data.humdata.org/dataset/cod-ab-uga.

Ohno, T., 2002. Fluorescence inner-filtering correction for determining the humification index of dissolved organic matter. Environ. Sci. Technol. 36, 742–746. https://doi.org/10.1021/es0155276.

Oksanen, J., Simpson, G.L., Blanchet, F.G., Kindt, R., Legendre, P., Minchin, P.R., O'hara, R., Solymos, P., Stevens, M.H.H., Szoecs, E., Wagner, H., Barbour, M., Bedward, M., 2025. _vegan: community ecology package_. In: R package version, 2, pp. 6–10. https://CRAN.R-project.org/package=vegan.

Osburn, C.L., Oviedo-Vargas, D., Barnett, E., Dierick, D., Oberbauer, S.F., Genereux, D.P., 2018. Regional groundwater and storms are hydrologic controls on the quality and

export of dissolved organic matter in two tropical rainforest streams, Costa Rica. J. Geophys. Res. Biogeosci. 123, 850–866. https://doi.org/10.1002/2017JG003960.
Owor, M., Taylor, R., Mukwaya, C., Tindimugaya, C., 2011. Groundwater/surface-water interactions on deeply weathered surfaces of low relief: evidence from Lakes Victoria and Kyoga, Uganda. Hydrogeol. J. 19, 1403.
Owor, M., Tindimugaya, C., Brown, L., Upton, K., Dochartaigh, Ó., Bellwood-Howard, 2018. Africa Groundwater Atlas: Hydrogeology of Uganda. British Geological Survey. https://earthwise.bgs.ac.uk/index.php/Hydrogeology_of_Uganda.
Parlanti, E., Wörz, K., Geoffroy, L., Lamotte, M., 2000. Dissolved organic matter fluorescence spectroscopy as a tool to estimate biological activity in a coastal zone submitted to anthropogenic inputs. Org. Geochem. 31, 1765–1781. https://doi.org/10.1016/S0146-6380(00)00124-8.
Pavlin, L., Széles, B., Strauss, P., Blaschke, A.P., Blöschl, G., 2021. Event and seasonal hydrologic connectivity patterns in an agricultural headwater catchment. Hydrol. Earth Syst. Sci. 25, 2327–2352. https://doi.org/10.5194/hess-25-2327-2021.
Pei, T., Qin, C.-Z., Zhu, A.-X., Yang, L., Luo, M., Li, B., Zhou, C., 2010. Mapping soil organic matter using the topographic wetness index: a comparative study based on different flow-direction algorithms and kriging methods. Ecol. Indic. 10, 610–619. https://doi.org/10.1016/j.ecolind.2009.10.005.
Quinn, P., Beven, K., Chevallier, P., Planchon, O., 1991. The prediction of hillslope flow paths for distributed hydrological modelling using digital terrain models. Hydrol. Process. 5, 59–79. https://doi.org/10.1002/hyp.3360050106.
Richards, L.A., Lapworth, D.J., Magnone, D., Gooddy, D.C., Chambers, L., Williams, P.J., van Dongen, B.E., Polya, D.A., 2019. Dissolved organic matter tracers reveal contrasting characteristics across high arsenic aquifers in Cambodia: a fluorescence spectroscopy study. Geosci. Front. 10, 1653–1667. https://doi.org/10.1016/j.gsf.2019.04.009.
Riihimäki, H., Kemppinen, J., Kopecký, M., Luoto, M., 2021. Topographic wetness index as a proxy for soil moisture: the importance of flow-routing algorithm and grid resolution. Water Resour. Res. 57. https://doi.org/10.1029/2021WR029871.
Rinderer, M., Van Meerveld, H., Seibert, J., 2014. Topographic controls on shallow groundwater levels in a steep, prealpine catchment: when are the TWI assumptions valid? Water Resour. Res. 50, 6067–6080. https://doi.org/10.1002/2013WR015009.
Rivett, M.O., Buss, S.R., Morgan, P., Smith, J.W., Bemment, C.D., 2008. Nitrate attenuation in groundwater: a review of biogeochemical controlling processes. Water Res. 42, 4215–4232. https://doi.org/10.1016/j.watres.2008.07.020.
Sacchi, E., Acutis, M., Bartoli, M., Brenna, S., Delconte, C.A., Laini, A., Pennisi, M., 2013. Origin and fate of nitrates in groundwater from the central Po plain: insights from isotopic investigations. Appl. Geochem. 34, 164–180. https://doi.org/10.1016/j.apgeochem.2013.03.008.
Sadeghi Goarbandi, F., Torangzar, H., Zare, R., Varvani, J., Ahmadi, A., 2024. Effects of landscape structure on river water characteristics: a multi-scale analysis. Int. J. Environ. Sci. Technol. 21, 8063–8080. https://doi.org/10.1007/s13762-024-05598-5.
Saito, T., Nishi, S., Amano, Y., Beppu, H., Miyakawa, K., 2023. Origin of dissolved organic matter in deep groundwater of marine deposits and its implication for metal binding. ACS ES&T Water 3, 4103–4112. https://doi.org/10.1021/acsestwater.3c00505.
Shen, Y., Chapelle, F.H., Strom, E.W., Benner, R., 2015. Origins and bioavailability of dissolved organic matter in groundwater. Biogeochemistry 122, 61–78. https://doi.org/10.1007/s10533-014-0029-4.
Shi, P., Zhang, Y., Li, Z., Li, P., Xu, G., 2017. Influence of land use and land cover patterns on seasonal water quality at multi-spatial scales. Catena 151, 182–190. https://doi.org/10.1016/j.catena.2016.12.017.
Song, Y., Song, X., Shao, G., Hu, T., 2020. Effects of land use on stream water quality in the rapidly urbanized areas: a multiscale analysis. Water 12. https://doi.org/10.3390/w12041123.
Sørensen, R., Zinko, U., Seibert, J., 2006. On the calculation of the topographic wetness index: evaluation of different methods based on field observations. Hydrol. Earth Syst. Sci. 10, 101–112. https://doi.org/10.5194/hess-10-101-2006.
Stegen, J.C., Fredrickson, J.K., Wilkins, M.J., Konopka, A.E., Nelson, W.C., Arntzen, E.V., Chrisler, W.B., Chu, R.K., Danczak, R.E., Fansler, S.J., Kennedy, D.W., Resch, C.T., Tfaily, M., 2016. Groundwater–surface water mixing shifts ecological assembly processes and stimulates organic carbon turnover. Nat. Commun. 7, 11237. https://doi.org/10.1038/ncomms11237.
Sugimura, Y., Suzuki, Y., 1988. A high-temperature catalytic oxidation method for the determination of non-volatile dissolved organic carbon in seawater by direct injection of a liquid sample. Mar. Chem. 24, 105–131. https://doi.org/10.1016/0304-4203(88)90043-6.
Taylor, R.G., Howard, K.W.F., 1996. Groundwater recharge in the Victoria Nile basin of east Africa: support for the soil moisture balance approach using stable isotope tracers and flow modelling. J. Hydrol. 180, 31–53. https://doi.org/10.1016/0022-1694(95)02899-4.
Taylor, P.G., Townsend, A.R., 2010. Stoichiometric control of organic carbon–nitrate relationships from soils to the sea. Nature 464, 1178–1181. https://doi.org/10.1038/nature08985.
Townsend-Small, A., McClelland, J.W., Max Holmes, R., Peterson, B.J., 2011. Seasonal and hydrologic drivers of dissolved organic matter and nutrients in the upper Kuparuk River, Alaskan Arctic. Biogeochemistry 103, 109–124. https://doi.org/10.1007/s10533-010-9451-4.
UBOS, 2024. National population and housing census. https://www.ubos.org/wp-content/uploads/publications/National-Population-and-Housing-Census-2024-Preliminary-Report.pdf.
UN-WWAP, 2006. Uganda National Water Development Report; Prepared for the 2nd UN World Water Development Report "Water a Shared Responsibility" UN-WATER, WWAP/2006/9. World Water Assessment Programme (WWAP).
UNEP, 2009. Uganda wetlands Atlas. https://www.unep.org/resources/report/uganda-wetlands-atlas-volume-ii.
UNMA, 2024. Monthly Outlook/Seasonal performance. https://meteo.mwe.go.ug/weather/seasonal-performance.
USAID-SWP, 2021. Uganda Water Resources Profile Overview. https://winrock.org/wp-content/uploads/2021/08/Uganda_Country_Profile_Final.pdf.
Weishaar, J.L., Aiken, G.R., Bergamaschi, B.A., Fram, M.S., Fujii, R., Mopper, K., 2003. Evaluation of specific ultraviolet absorbance as an indicator of the chemical composition and reactivity of dissolved organic carbon. Environ. Sci. Technol. 37, 4702–4708. https://doi.org/10.1021/es030360x.
Williams, C.J., Frost, P.C., Morales-Williams, A.M., Larson, J.H., Richardson, W.B., Chiandet, A.S., Xenopoulos, M.A., 2016. Human activities cause distinct dissolved organic matter composition across freshwater ecosystems. Glob. Change Biol. 22, 613–626. https://doi.org/10.1111/gcb.13094.
Williams, C.J., Yamashita, Y., Wilson, H.F., Jaffé, R., Xenopoulos, M.A., 2010. Unraveling the role of land use and microbial activity in shaping dissolved organic matter characteristics in stream ecosystems. Limnol. Oceanogr. 55, 1159–1171. https://doi.org/10.4319/lo.2010.55.3.1159.
Wilson, G.J., Hamisi, R., Denwood, T., Muloogi, D., Bhattacharya, P., Nuwategeka, E., Gooddy, D.C., Polya, D.A., Huck, J.J., Richards, L.A., 2024a. *Geochemical Tracers Reveal urban-derived Contamination of Groundwater and Springs in Gulu City, Uganda. Presented at the EGU General Assembly Conference Abstracts, p. 9232.
Wilson, G.J., Muloogi, D., Hamisi, R., Denwood, T., Bhattacharya, P., Nuwategeka, E., Gooddy, D.C., Polya, D.A., Huck, J.J., Richards, L.A., 2024b. Surface-derived groundwater contamination in Gulu District, Uganda: chemical and microbial tracers. Sci. Total Environ. 955, 177118. https://doi.org/10.1016/j.scitotenv.2024.177118.
Wilson, G.J.L., Aind, D.A., Mukherjee, A., Polya, D.A., Gooddy, D.C., Richards, L.A., 2025. Monsoonal rainfall initiates autochthonous alteration of dissolved organic matter composition in Indian groundwaters. Appl. Geochem., 106298 https://doi.org/10.1016/j.apgeochem.2025.106298.
Wilson, G.J.L., Lu, C., Lapworth, D.J., Kumar, A., Ghosh, A., Niasar, V.J., Krause, S., Polya, D.A., Gooddy, D.C., Richards, L.A., 2023. Spatial and seasonal controls on dissolved organic matter composition in shallow aquifers under the rapidly developing city of Patna, India. Sci. Total Environ. 903, 166208. https://doi.org/10.1016/j.scitotenv.2023.166208.
Wilson, H.F., Xenopoulos, M.A., 2009. Effects of agricultural land use on the composition of fluvial dissolved organic matter. Nat. Geosci. 2, 37–41. https://doi.org/10.1038/ngeo391.
Xenopoulos, M.A., Barnes, R.T., Boodoo, K.S., Butman, D., Catalán, N., D'Amario, S.C., Fasching, C., Kothawala, D.N., Pisani, O., Solomon, C.T., Spencer, R.G.M., Williams, C.J., Wilson, H.F., 2021. How humans alter dissolved organic matter composition in freshwater: relevance for the Earth's biogeochemistry. Biogeochemistry 154, 323–348. https://doi.org/10.1007/s10533-021-00753-3.
Yamashita, Y., Jaffé, R., Maie, N., Tanoue, E., 2008. Assessing the dynamics of dissolved organic matter (DOM) in coastal environments by excitation emission matrix fluorescence and parallel factor analysis (EEM-PARAFAC). Limnol. Oceanogr. 53, 1900–1908. https://doi.org/10.4319/lo.2008.53.5.1900.